RICE UNIVERSITY

ONE DIMENSIONAL SHEAR MOTIONS IN FLUID SATURATED POROUS MEDIA

by

Kyle R. Roberson

A THESIS SUBMITTED
IN PARTIAL FULFILLMENT OF THE
REQUIREMENTS FOR THE DEGREE

MASTER OF SCIENCE

APPROVED, THESIS COMMITTEE:

Ray M. Bowen
Professor of Mechanical Engineering
Chairman

James C. Wilhoit, Jr.
Professor of Mechanical Engineering

C. C. Wang
Professor of Mathematical Sciences

HOUSTON, TEXAS

MAY 1981

ABSTRACT

ONE DIMENSIONAL SHEAR MOTIONS IN FLUID SATURATED POROUS MEDIA

by Kyle R. Roberson

An analytic solution is presented for shear motions in a binary mixture of a chemically inert, isothermal, elastic isotropic solid and elastic fluid subject to a sinusoidally varying solid displacement on one boundary and free of tractions on the other. It is demonstrated that the retention of inertial terms, and the resulting resonance phenomenon, can cause solid displacements in the interior of the region orders of magnitude greater than the exciting solid displacement on the boundary. Displacement spectra are presented for certain well known porous media.

ACKNOWLEDGEMENTS

I would like to acknowledge the guidance and assistance given to me by the faculty and staff of Rice University, especially to my advisor, Prof. Bowen, and the members of my committee. My attendance at Rice and the writing of this thesis was made possible by a Rice Fellowship for two years, and by a Weyerhaeuser Fellowship for a third.

In addition, I would like to thank my parents for their generous support, and though I can't say my wife typed the manuscript of this work she did contribute to its completion. Finally, I had wanted to mention my son, Stellan, but I felt that it might be unfair to mention him and not the baby due in June.

LIST OF SYMBOLS

$\mathbf{T}$	Stress tensor
$\mathbf{E}_s$	Infinitesimal strain measure for solid
$\mathbf{w}_f$	Fluid displacement vector
$\mathbf{w}_s$	Solid displacement vector
ξ	Drag coefficient
μ_s	Solid shear modulus
ϕ_f	Porosity, volume occupied by fluid
μ_f	Fluid viscosity
P_f	Pore pressure
ρ_f	Fluid bulk density
ρ_s	Solid bulk density
γ_f	Fluid true density
γ_s	Solid true density
u_3	Solid transverse acceleration wave speed
u_0	Frozen wave speed
ω_0	Reciprocal characteristic time for diffusion
ω_*	Reciprocal time
ϕ	Frequency applied to the boundary
L	Formation depth
x	Position in formation
n	index
γ_n	$(2n-1)\pi/L$
e_n	$u_0\gamma_n/\omega_0$
q	Used in calculations of cubic roots
r	" "
S_1	" "
S_2	" "
s_1	Real root of cubic
$s_{2,3}$	Complex conjugate root of cubic
ξ_n	$\lvert s_1 \rvert$ for each n
ζ_n	$\lvert \mathbf{R}(s_{2,3}) \rvert$ for each n

ω_n	$\lvert I(s_{2,3})\rvert$ for each n
$g(s)$	$s\sqrt{\frac{s+\omega_0}{s+\omega_*}}$
$c(\phi)$	Real part of g(s)
$d(\phi)$	Imaginary part of g(s)
ϕ_{res}	Steady-state resonant frequency
$(\dot{\ })$	Partial derivative with respect to time
$(\bar{\ })$	Laplace Transform
$()_{ss}$	Steady-state component
$()_{md}$	Monotonic-decaying component
$()_{cd}$	Cyclic-decaying component

LIST OF FIGURES AND TABLES

2.1 Contour Used in Inverting Transform.....12

2.2 The Domain for the Fuction g(s)
its Derivative..........................23

3.1 Berea Sandstone:
Material Properties, Decay Exponents
and Resonant Frequencies................44

3.2 Berea Sandstone: Maximum Displacement
and T_{max} at φ=.999 ω_n..................46

3.3 Berea Sandstone: Displacement Spectra
Near $\varphi = \omega_1$.............................47

3.4 Ruhr Sandstone:
Material Properties, Decay Exponents
and Resonant Frequencies................49

3.5 Ruhr Sandstone: Maximum Displacement
and T_{max} at φ=.999 ω_n..................51

3.6 Ruhr Sandstone: Displacement Spectra
Near $\varphi = \omega_1$.............................52

TABLE OF CONTENTS

Abstract....................................ii
Acknowledgements............................iii
List of Symbols..............................iv
List of Figures..............................vi

I. Introduction................................1
1.1 Field and Constitutive Equations........2
1.2 Wave Speeds and Characteristic Time.....3
1.3 Elastic and Drag Coefficients...........4
1.4 Uniqueness and Boundary Conditions......4
1.5 Comparison to Classical Biot Model......6

II. 2.1 Method of Solution.....................7
2.2 Calculation of the Poles...............10
2.3 Residue Theorem........................11
2.4 Determination of the Poles.............13
2.5 Closed Form Solution for the Poles....15
2.6 Proof that the Discriminant is ≥ 0....16
2.7 Approximations to the Roots...........19
2.8 Principle of Reflection...............21
2.9 Complete Solution to Equation 2.1.29..24
2.10 Steady-State Component................25
2.11 Monotonic-Decaying Component..........28
2.12 Cyclic-Decaying Component.............30
2.13 Total Response........................33

III. Introduction..............................34
3.1 List of Computer Notation.............36
3.2 List of Subroutines...................38
3.3 Flow Chart of Program RESO............40
3.4 Displacement Spectra..................41

3.4.1 Results for Berea Sandstone..........42
3.4.2 Results for Ruhr Sandstone...........48
3.5 Conclusions.............................53

Bibliography................................54

Appendix....................................56
Listing of Program RESO

CHAPTER I

THE POROUS MEDIA MODEL

Introduction

In this thesis, the dynamic behavior of a binary mixture of a chemically inert, isothermal, elastic isotropic solid and elastic fluid restricted to shear motions is presented. The porous media is assumed to be excited from below by a sinusoidally varying displacement and bounded by a stress free surface on top. This thesis is predicated on the equations derived by BOWEN[1], which are a generalization of those obtained by BIOT[3]. The phenomenon of resonance, due to the presence of inertial terms, is demonstrated to be of importance in the dynamic behavior of porous media.

The work is divided into three chapters. The present chapter contains a statement of the field equations and constitutive equations and a summary of the parameters contained therein. Chapter II presents the transient and steady-state components of the solution of the equations for a specified set of boundary-initial conditions. Chapter III contains a discussion of an implementation of the solution on a computer, and results are presented for certain porous media in the form of displacement spectra.

Section 1.1 Field and Consitutive Equations

BOWEN[1] shows that the field equations for a binary mixture of a chemically inert, isothermal, elastic isotropic solid and elastic fluid are, in the absence of body forces and restricted to shear motions:

$$\rho_f \ddot{w}_f = -\xi(\dot{w}_f - \dot{w}_s) \qquad 1.1.1$$

and

$$\rho_s \ddot{w}_s = \mu_s \operatorname{div} \operatorname{grad} w_s + \xi(\dot{w}_f - \dot{w}_s). \qquad 1.1.2$$

The constitutive equation for stress is

$$T = 2\mu_s E_s. \qquad 1.1.3$$

Definitions of all the symbols used in this thesis may be found preceding the Table of Contents.

If the restriction to one spatial dimension is added by choosing

$$w_f \equiv (0,0,w_f(x,t)) \qquad 1.1.4$$

and

$$w_s \equiv (0,0,w_s(x,t)), \qquad 1.1.5$$

the field equations become

$$\rho_f \ddot{w}_f = -\xi(\dot{w}_f - \dot{w}_s) \qquad 1.1.6$$

and

$$\rho_s \ddot{w}_s = \mu_s \frac{\partial^2 w_s}{\partial x^2} + \xi(\dot{w}_f - \dot{w}_s). \qquad 1.1.7$$

The constitutive equation for stress is now

$$T_{13} = T_{31} = \mu_s \frac{\partial w_s}{\partial x}. \qquad 1.1.8$$

The field equations 1.1.6,7 are solved in Chapter II.

Section 1.2 Wave Speeds and Characteristic Time

BOWEN[1] discusses acceleration wave speeds for porous media. The transverse wave speed for the mixture is there shown to be

$$u_3^2 \equiv \frac{\mu_s}{\rho_s}\,. \qquad 1.2.9$$

Another squared speed which is important is the frozen wave speed u_0. It is called the frozen wave speed because it arises naturally in the solution of the equations when the drag coefficient, ξ , approaches infinity. For shear motions only, u_0 is defined by

$$u_0^2 \equiv \frac{\mu_s}{\rho_f + \rho_s}\,. \qquad 1.2.10$$

The final parameter to be introduced is

$$\omega_0 \equiv \xi\left(\frac{1}{\rho_f} + \frac{1}{\rho_s}\right), \qquad 1.2.11$$

which is a reciprocal time characteristic of diffusion in the mixture. The parameter is important since it defines what is meant by a "long-time" (with respect to diffusion) solution. Similarly, when in the sequel a frequency ϕ is referred to as small or low, what is meant is

$$\frac{\phi}{\omega_0} << 1. \qquad 1.2.12$$

Section 1.3 Elastic and Drag Coefficients

The material properties used here, apart from the density, are taken from RICE AND CLEARY[2], which has the properties of several porous media given in tabular form. The necessary parameters and their notation in RICE AND CLEARY[2] are: the shear modulus μ_s, denoted by G, the porosity ϕ_f , denoted by v_0, and the drag coefficient which is calculated from

$$\xi = \frac{\phi_f^2 \mu_f}{k} = \frac{v_0^2 \mu_f}{k} , \qquad 1.3.13$$

where μ_f is the viscosity of the fluid and k is the permeability of the mixture.

The bulk density of the solid is taken from FARMER[10] and is denoted by ρ_s. A true density, γ_s or γ_f, must be multiplied by the volume fraction occupied by that material to get the bulk density ρ_s or ρ_f.

Section 1.4 Uniqueness and Initial-Boundary Conditions

Uniqueness is assured if (BOWEN[1], SCHNEIDER[5])

$$\xi \geq 0 \qquad 1.4.14$$

and

$$\mu_s > 0. \qquad 1.4.15$$

The restriction on the drag coefficient is a consequence of the entropy inequality, and the restriction on the shear modulus is a result of requiring the shear strain energy to be positive definite.

The porous media is considered to be at rest at t=0, and with initial displacements taken as zero. Thus,

$$w_f(x,0) = 0, \qquad 1.4.16$$

$$\dot{w}_f(x,0) = 0, \qquad 1.4.17$$

$$w_s(x,0) = 0 \qquad 1.4.18$$

and

$$\dot{w}_s(x,0) = 0. \qquad 1.4.19$$

The boundary conditions are as follows: no shear stress at x=0 and specification of the solid displacement at x=L. Thus,

$$\left.\frac{\partial w_s(x,t)}{\partial x}\right|_{x=0} = 0 \qquad 1.4.20$$

and

$$w_s(L,t) = W \sin\phi t. \qquad 1.4.21$$

Section 1.5 Comparison to Classical Biot Model

The equations used herein are similar to those derived by BIOT[3] with two exceptions, BOWEN[1]: Biot included virtual mass effects which are neglected here, but the equations do include buoyancy effects which Biot's did not. These differences are not significant in the context of this thesis which is particularly concerned with inertial effects.

CHAPTER II

ONE DIMENSIONAL SHEAR MOTIONS IN FLUID SATURATED POROUS MEDIA

Section 2.1 Method of Solution

The method used to solve equations 1.1.6,7 with the boundary conditions 1.4.7,8 and the initial conditions 1.4.3-6 is the method of Laplace Transforms. CHURCHILL [8] defines the Laplace Transform by

$$\bar{w}(x,s) \equiv \int_0^\infty e^{-st} w(x,t)\, dt, \qquad 2.1.22$$

where the transform parameter s is in general complex. Under fairly general conditions, the integral above can be said to converge, usually in some half-plane $R(s)>|x_0|$. In this half-plane, the transform is analytic and of exponential order. In the present case, the solution in the transform space will turn out to be analytic and of exponential order in the half-plane $R(s)>0$.

With the use of the initial conditions 1.4.3-6, equations 1.1.6,7 are transformed to

$$\rho_f \bar{w}_f s^2 = -\xi s(\bar{w}_f - \bar{w}_s) \qquad 2.1.23$$

and

$$\rho_s \bar{w}_s s^2 = \mu_s \frac{d^2\bar{w}_s}{dx^2} + \xi s(\bar{w}_f - \bar{w}_s). \qquad 2.1.24$$

The first equation may be solved for $\bar{w}_f$ in terms of $\bar{w}_s$.

The result is

$$\bar{w}_f = \frac{\xi}{\rho_f s + \xi}\,\bar{w}_s = \frac{\bar{w}_s}{\left[\frac{u_3}{u_0}\right]^2 \frac{s}{\omega_0} + 1}, \qquad 2.1.25$$

where equations 1.2.9-11 have been used.

Substitution of equation 2.1.25 into equation 2.1.24 results in the following ordinary differential equation for $\bar{w}_s$:

$$\frac{d^2\bar{w}_s}{dx^2} = \frac{1}{u_3^2}\, s^2 \left[\frac{s + \omega_0}{s + \omega_*}\right] \bar{w}_s, \qquad 2.1.26$$

where

$$\omega_* \equiv \left[\frac{u_0}{u_3}\right]^2 \omega_0. \qquad 2.1.27$$

The solution of the above ordinary differential equation is straight forward. The transformed solid displacement is

$$\bar{w}_s = A \cosh\left[\frac{x}{u_3} s \sqrt{\frac{s + \omega_0}{s + \omega_*}}\right] + B \sinh\left[\frac{x}{u_3} s \sqrt{\frac{s + \omega_0}{s + \omega_*}}\right]. \qquad 2.1.28$$

Application of the transform of the boundary conditions 1.4.7,8 reduces equation 2.1.28 to the following result

$$\bar{w}_s = \frac{W\phi}{s^2 + \phi^2} \quad \frac{\cosh\left[\frac{x}{u_3} g(s)\right]}{\cosh\left[\frac{L}{u_3} g(s)\right]}, \qquad 2.1.29$$

where

$$g(s) \equiv s \sqrt{\frac{s + \omega_0}{s + \omega_*}} \quad . \qquad 2.1.30$$

Since the actual value of w_f is of little practical value, it is not calculated explicitly. It may, however, be expressed as a convolution integral of the solution w_s

$$w_f = \int_0^t \omega_* \, e^{-\omega_*(t-u)} \, w_s(x,u) \, du, \qquad 2.1.31$$

where the convolution theorem for Laplace Transforms and equation 2.1.25 have been used.

From the point of view of inversion of the Laplace Transform, the most important aspect of the solution 2.1.29 is that despite the appearance of the radical g(s) as an argument in the hyperbolic functions, the solutions are analytic everywhere except at a countable number of poles. These poles are first order. Thus the Residue Theorem may be readily applied to invert $\bar{w}_s(x,s)$ to obtain $w_s(x,t)$.

To demonstrate that there are no branch cuts in the solution 2.1.29, the series representation of coshx is used

$$\cosh x = 1 + \frac{x^2}{2!} + \frac{x^4}{4!} + \ldots \qquad 2.1.32$$

Note that coshx contains only even powers of the argument, and since

$$g^2(s) = s^2 \, \frac{s + \omega_0}{s + \omega_*} \qquad 2.1.33$$

is single valued, there is no branch cut involved. Finally, since the quotient of two convergent power series in s is analytic except where the denominator vanishes, the solution 2.1.29 is analytic everywhere except at the zeros of the denominator.

Section 2.2 Calculation of the Poles

In order to use the Residue Theorem, it will be necessary to obtain the zeros of the associated cosh function

$$\cosh\left[\frac{L}{u_3}g(s)\right] = 0. \qquad 2.2.34$$

The zeros are calculated easily from the following identity

$$\cosh(iz)=\cos(z). \qquad 2.2.35$$

Therefore, the zeros of equation 2.2.34 are

$$g(s) = \pm i\left\{\frac{2n-1}{2}\frac{\pi}{L}\right\}u_3 = \pm i\gamma_n u_3, \quad n = 1,2,3,\ldots \qquad 2.2.36$$

One must, therefore, solve an equation of the form

$$s^3 + \omega_0 s^2 + u_3^2\gamma_n^2 s + \gamma_n^2 u_0^2\omega_0 = 0 \qquad 2.2.37$$

to obtain s. Equation 2.2.37 is derived from equation 2.2.36 by squaring both sides and clearing fractions. These manipulations preserve the solutions of the original equations, but extraneous solutions could be introduced. In the following it is shown that such roots are not introduced.

Assume that a solution η of equation 2.2.37 is found such that

$$g(\eta) = \kappa \neq \pm i\gamma_n u_3. \qquad 2.2.38$$

It follows from 2.2.38 that η also satisfies

$$\eta^3 + \omega_0\eta^2 - \kappa^2\eta - \kappa^2\omega_* = 0. \qquad 2.2.39$$

Because η is also a solution of 2.2.37, if 2.2.39 is subtracted from 2.2.37 it follows that

$$(u_3^2\gamma_n^2 + \kappa^2)(\eta + \omega_*) = 0. \qquad 2.2.40$$

Obviously,

$$\eta \neq -\omega_* \qquad 2.2.41$$

by inspection of either equation 2.2.36 or 2.2.37. Hence,

$$\kappa = \pm i\gamma_n u_3 \qquad 2.2.42$$

which contradicts the original assumption. Consequently, all solutions of the associated cubic equation 2.2.37 are solutions of 2.2.36.

Section 2.3 Residue Theorem

CHURCHILL [8] defines the inverse Laplace Transform as

$$w_s(x,t) = \frac{1}{2\pi i}\int_{\gamma-i\infty}^{\gamma+i\infty} e^{st}\,\bar{w}_s(x,s)\,ds \qquad 2.3.43$$

where the function $\bar{w}_s(x,s)$ is analytic everywhere in the half-plane $R(s) > \gamma$. Further, it can be shown that if $\bar{w}_s$ is of exponential order then

$$w_s(x,t) = \frac{1}{2\pi i}\oint_C e^{st}\,\bar{w}_s(x,s)\,ds = \sum \text{residues inside C.} \qquad 2.3.44$$

The contour C is chosen such that it is the limiting curve of C_m in figure 2.1 as $R_m \to \infty$, and so that C_m does not intersect any of the poles.

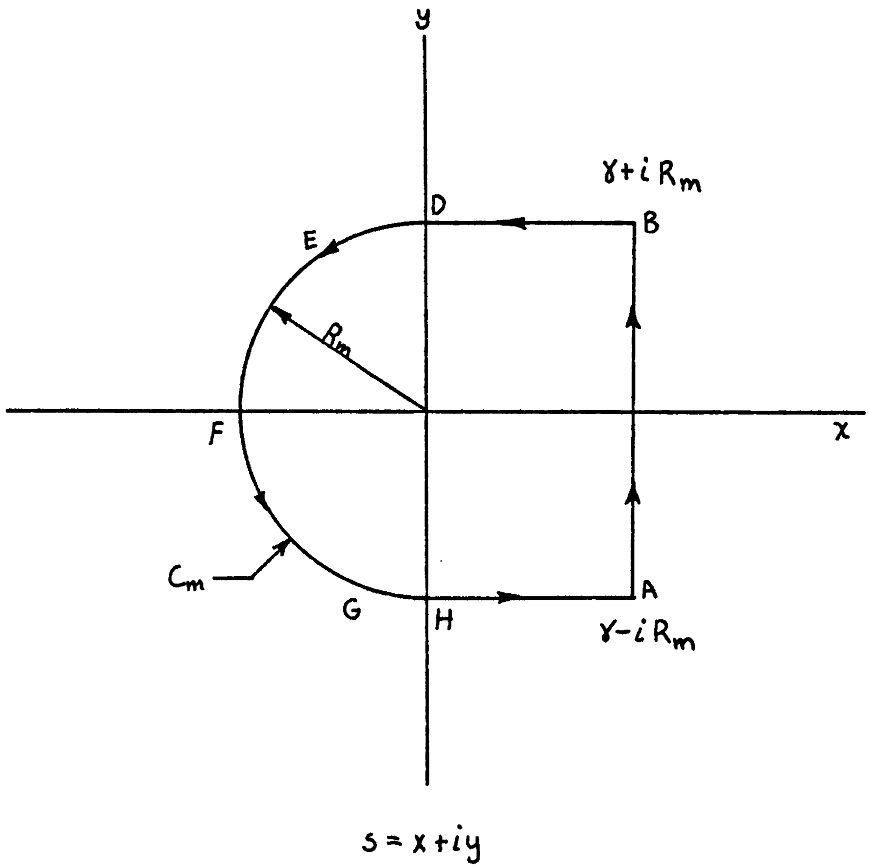

Contour Used in Inverting Transform

Figure 2.1

In the next section, by use of a standard result from the theory of equations, any solution of equation 2.2.37 will be shown to have negative real part. Thus the poles of the hyperbolic functions will lie in the half-plane $R(s)<0$ (with $\gamma_n^2 > 0$), and the residues of these poles will represent transient, exponentially decaying components of $w_s(x,t)$. The poles of $1/(s^2+\phi^2)$ lie on the line $R(s)=0$. Therefore, γ as defined in figure 2.1 is any number $x_0>0$.

Section 2.4 Determination of the Poles

USPENSKY[4] contains a proof of the following theorem, called the Routh-Hurwitz Theorem: A polynomial

$$P^n(x) \equiv p_0 + p_1 x + p_2 x^2 + \dots + p_n x^n = 0 \qquad 2.4.45$$

has roots with negative real part, provided that the coefficients are real (if necessary, the constant term is made positive by multiplying through by minus one before beginning), if and only if the n determinants which follow are positive definite.

$$D_1 \equiv p_1 > 0, \qquad 2.4.46$$

$$D_2 \equiv \begin{vmatrix} p_1 & p_0 \\ p_3 & p_2 \end{vmatrix} > 0, \qquad 2.4.47$$

$$D_3 \equiv \begin{vmatrix} p_1 & p_0 & 0 \\ p_3 & p_2 & p_1 \\ p_5 & p_4 & p_3 \end{vmatrix} > 0, \dots \qquad 2.4.48$$

and

$$D_n \equiv \begin{vmatrix} p_1 & p_0 & \cdots & 0 \\ p_3 & p_2 & \cdots & 0 \\ \cdots & \cdots & \cdots & \cdots \\ p_{2n-1} & \cdots & & p_n \end{vmatrix} > 0. \qquad 2.4.49$$

For a cubic, one obtains

$$p_0 > 0, \qquad 2.4.50$$

$$p_1 > 0, \qquad 2.4.51$$

$$p_1 p_2 - p_0 p_3 > 0 \qquad 2.4.52$$

and

$$p_3(p_1 p_2 - p_0 p_3) > 0. \qquad 2.4.53$$

From equation 2.2.37, the necessary conditions are

$$\gamma_n^2 u_0 \omega_0 > 0, \qquad 2.4.54$$

$$u_3^2 \gamma_n^2 > 0 \qquad 2.4.55$$

and

$$\omega_0 \gamma_n^2 \left(1 - \left[\frac{u_0}{u_3}\right]^2\right) > 0. \qquad 2.4.56$$

The above inequalities are all satisfied provided $\gamma_n^2 \neq 0$. This assertion is true because, from equations 1.2.9-11, $\omega_0 > 0$, $u_0 > 0$ and $u_3 > u_0$.

If $\gamma_n^2 = 0$, then $s=0$ or $s=-\omega_0$, where the root $s=0$ has multiplicity 2. This possibility occurs only in the case n=0 which is not encountered here. Therefore, all non-trivial roots have negative real part.

Notice that equation 2.2.36 evaluates to a real number if s is real. Thus, if s is real and a solution of 2.2.37, then from equation 2.2.36

$$\frac{s + \omega_0}{s + \omega_*} < 0. \qquad 2.4.57$$

Therefore, any real root to equation 2.2.37 must lie in the range

$$-\omega_0 < s < -\omega_*. \qquad 2.4.58$$

Bounds for the real part of the complex solutions are derived in Section 2.7.

Section 2.5 Closed Form Solution for the Poles

The exact solution of equation 2.2.37 can be obtained by formula. In almost any handbook or algebra text, one can find the following formulae or their equivalent. Let

$$q \equiv \frac{u_3^2 \gamma_n^2}{3} - \left(\frac{\omega_0}{3}\right)^2 , \qquad 2.5.59$$

$$r \equiv \frac{1}{2}(\omega_0 u_3^2 \gamma_n^2 (\frac{1}{3} - \left(\frac{u_0}{u_3}\right)^2)) - \left(\frac{\omega_0}{3}\right)^3 , \qquad 2.5.60$$

$$S_1 \equiv (r + \sqrt{q^3 + r^2})^{1/3} \qquad 2.5.61$$

and

$$S_2 \equiv (r - \sqrt{q^3 + r^2})^{1/3} . \qquad 2.5.62$$

It is shown in the sequel that, except for the trivial case $\gamma_n^2 = 0$, the quantity $q^3 + r^2$ (called the discriminant) is always positive. Thus, there is one real root and one complex conjugate pair. The roots are (regardless of the sign of $q^3 + r^2$):

$$s_1 = S_1 + S_2 - \omega_0/3 , \qquad 2.5.63$$

$$s_2 = -\frac{1}{2}(S_1 + S_2) - \omega_0/3 + i\frac{\sqrt{3}}{2}(S_1 - S_2) \qquad 2.5.64$$

and

$$s_3 = -\frac{1}{2}(S_1 + S_2) - \omega_0/3 - i\frac{\sqrt{3}}{2}(S_1 - S_2). \qquad 2.5.65$$

It must be pointed out that in the present application these formulae require the addition and subtraction of numbers quite different in magnitude. To avoid round-off-errors which can swamp the actual solutions, a numerical solution is employed. There are several methods adequate for this purpose, and one of the simpler methods is the Lin-Bairstow Algorithm, HOVANESSIAN AND PIPES[11]. This method calculates the complex roots without explicitly carrying out complex arithmetic. The Lin-Bairstow Algorithm is used in Chapter III to calculate the roots of equation 2.2.37.

Section 2.6 Proof that the Discriminant is ≥ 0

The character of the solutions of any cubic equation can be determined by examining the discriminant q^3+r^2. If it is greater than zero, then there is one real and one complex conjugate pair. If it is equal to zero, then all roots are real and at least two are equal. In the last remaining case, the discriminant is less than zero, and there are three real and distinct roots. With ω_0, u_0, and u_3 fixed, q^3+r^2 is a function of γ_n^2. The discriminant at $\gamma_n^2=0$ is

$$(q^3 + r^2)(0) = -\left(\frac{\omega_0}{3}\right)^6 + \left(\frac{\omega_0}{3}\right)^6 = 0. \qquad 2.6.66$$

The derivative of the discriminant with respect to γ_n^2 at $\gamma_n^2 = 0$ yields

$$\frac{d}{d\gamma_n^2}(q^3 + r^2) = q^2u_3^2 + r(\omega_0 u_3^2(\tfrac{1}{3} - \left(\frac{u_0}{u_3}\right)^2)), \qquad 2.6.67$$

and at $\gamma_n^2 = 0$

$$\frac{d}{d\gamma_n^2}(q^3 + r^2) .= \omega_0 u_0^2 \left(\frac{\omega_0}{3}\right)^3 > 0. \qquad 2.6.68$$

Hence, at $\gamma_n^2 = 0^+$ (where the superscript + means slightly greater than zero), q^3+r^2 is greater than zero and increasing. It will now be shown that the other roots of

$$q^3 + r^2 = 0 \qquad 2.6.69$$

have negative real part. Thus for $\gamma_n^2 > 0$, equation 2.2.37 will have one real root and one complex conjugate pair.

Equation 2.2.37 can be written as

$$x^3 + x^2 \; a^2b^2x + b^2 = 0, \qquad 2.6.70$$

where

$$x \equiv s/\omega_0, \qquad 2.6.71$$

$$a \equiv u_3/u_0 \qquad 2.6.72$$

and

$$b \equiv \frac{u_0\gamma_n}{\omega_0} \; . \qquad 2.6.73$$

The quantities q and r are then

$$q = \frac{a^2b^2}{3} - \left(\frac{1}{3}\right)^2 \qquad 2.6.74$$

and

$$r = \frac{1}{2}\left(\frac{a^2b^2}{3} - b^2\right) - \left(\frac{1}{3}\right)^3 . \qquad 2.6.75$$

The discriminant is now set equal to zero, and the resulting equation can be factored as

$$b^2\left(b^4 - \frac{27}{a^6}\left(1 - \frac{2}{9}a^2 - \frac{a^4}{108}\right)b^2 + \frac{1}{a^6}\right) = 0. \qquad 2.6.76$$

The roots of the above equation will have negative real part, apart from the trivial root $b^2=0$, if, by the results of Section 2.4,

$$\left(\frac{1}{a}\right)^6 > 0 \qquad 2.6.77$$

and

$$\frac{-27}{a^6}\left(1 - \frac{2}{9}a^2 - \frac{a^4}{108} \right) > 0. \qquad 2.6.78$$

The first inequality is satisfied by definition, the second is satisfied if

$$a^4 + 24a^2 - 108 > 0. \qquad 2.6.79$$

The above equation can be solved to yield $a^2 > -6$ or -18. This is clearly always the case, therefore, there are no zeros of the discriminant for $b^2>0$ which implies there are none for $\gamma_n^2>0$. Thus, the discriminant is positive definite as a function of γ_n^2.

Section 2.7 Approximations to the Roots

Given equation 2.2.37, the following two dimensionless equations can be formed

$$\left(\frac{s}{\omega_0}\right)^3 + \left(\frac{s}{\omega_0}\right)^2 + \left(\frac{u_3}{u_0}\right)^2 e_n^2\left(\frac{s}{\omega_0}\right) + e_n^2 = 0 \qquad 2.7.80$$

and

$$\left(\frac{s}{u_0\gamma_n}\right)^3 + \frac{1}{e_n}\left(\frac{s}{u_0\gamma_n}\right)^2 + \left(\frac{u_3}{u_0}\right)^2\left(\frac{s}{u_0\gamma_n}\right) + \frac{1}{e_n} = 0, \qquad 2.7.81$$

where

$$e_n \equiv \frac{u_0\gamma_n}{\omega_0} \quad . \qquad 2.7.82$$

Thus in the case $e_n \ll 1$, the solution to 2.2.80 can be written as the power series

$$\left(\frac{s}{\omega_0}\right) = \sum_{m=0}^{\infty} a_m e_n^m, \qquad 2.7.83$$

and when $e_n \gg 1$ the solution to 2.7.81 can be written as

$$\left(\frac{s}{u_0\gamma_n}\right) = \sum_{m=0}^{\infty} a_m (1/e_n^m) . \qquad 2.7.84$$

Typically, the two solutions correspond to n small and n large.

Substitution of the series 2.7.83 into equation 2.7.80 yields the following restrictions on a_m:

$$(e_n^0) \quad a_0^2(a_0 + 1) = 0, \qquad 2.7.85$$

$$(e_n^1) \quad a_1 a_0(3a_0 + 2) = 0, \qquad 2.7.86$$

and

$$(e_n^2) \quad 3a_0{}^2a_2 + 3a_0a_1^2 + 2a_0a_2 + a_1^2 + (u_3/u_0)^2 a_0 + 1 = 0. \qquad 2.7.87$$

Solving the first equation for a_0 gives a_0=0,0, or -1. If a_0=0, then

$$a_1 = \pm i \tag{2.7.88}$$

and

$$a_2 = \frac{1}{2}\left(1 - (u_3/u_0)^2\right). \tag{2.7.89}$$

Thus the solution for s is

$$s_{2,3} = \frac{1}{2}\,\frac{u_0^2 - u_3^2}{\omega_0}\,\gamma_n^2 \pm i\gamma_n u_0 + O(e_n^3). \tag{2.7.90}$$

If a_0=-1, then a_1=0 and

$$a_2 = (u_3/u_0)^2 - 1. \tag{2.7.91}$$

So the solution for s in this case is

$$s_1 = -\omega_0 + \frac{u_3^2 - u_0^2}{\omega_0}\,\gamma_n^2 + O(e_n^3). \tag{2.7.92}$$

Therefore, the roots of equation 2.2.37 are approximated by 2.7.90 and 2.7.92 when $e_n \ll 1$.

When $e_n \gg 1$, substitution of the series 2.7.84 into equation 2.7.81 yields the following set of restrictions on a_m:

$$(1/e_n^0)\quad a_0(a_0^2 + (u_3/u_0)^2) = 0, \tag{2.7.93}$$

$$(1/e_n^1)\quad a_0^2 + 3a_0^2a_1 + (u_3/u_0)^2a_1 + 1 = 0 \tag{2.7.94}$$

and

$$(1/e_n^2)\quad (u_3/u_0)^2a_2 + 2a_0a_1 + (a_0(2a_0a_2 + a_1^2) + a_1(2a_0a_1) + a_2a_0^2) = 0. \tag{2.7.94B}$$

Solving the first equation for a_0 gives a_0=0, $\pm i(u_3/u_0)$. If

$a_0=0$, then $a_1=-(u_0/u_3)^2$ and $a_2=0$. Therefore, the solution for s is

$$s_1 = -\omega_* + O(1/e_n^3). \qquad 2.7.95$$

If $a_0= \pm i(u_3/u_0)$, then

$$a_1 = -\frac{1}{2}(1 - (u_0/u_3)^2). \qquad 2.7.96$$

So the solution for s is

$$S_{2,3} = -\frac{1}{2}(1 - (u_0/u_3)^2)\omega_0 \pm i\gamma_n u_3 + O(1/e_n^2). \qquad 2.7.97$$

The error in the real part of 2.7.97 is third order. These approximations to the roots when $e_n >> 1$ can be used to give bounds on the roots as $n \to \infty$. The real root approximated by 2.7.95 approaches $-\omega_*$, the upper bound of the range derived earlier for the real root. The real part of the approximation 2.7.97 is bounded below by the midpoint of the same range. The imaginary part of 2.7.97 is unbounded as n becomes infinitely large.

Section 2.8 Principle of Reflection

It will be necessary later to use the fact that the function g(s), defined by equation 2.1.30, has the following property

$$g(\bar{s}) = \overline{g(s)} \qquad 2.8.98$$

and

$$g'(\bar{s}) = \overline{g'(s)}. \qquad 2.8.99$$

Most textbooks on complex variables contain a proof of the following theorem (see for example CHURCHILL, BROWN AND

VERHEY[9]).

Let a function f be analytic in some domain D that includes a segment of the real axis and is symmetric to the real axis. If f(x) is real whenever x is a point on that segment, then

$$f(\bar{z}) = \overline{f(z)} \tag{2.8.100}$$

whenever z is a point in D.

To satisfy these conditions, define the domain as the complex plane with a branch cut along the real axis. A point x is on the branch cut if

$$-\omega_0 < x \leqq -\omega_*. \tag{2.8.101}$$

See figure 2.2. for an illustration of the domain and location of the branch cut.

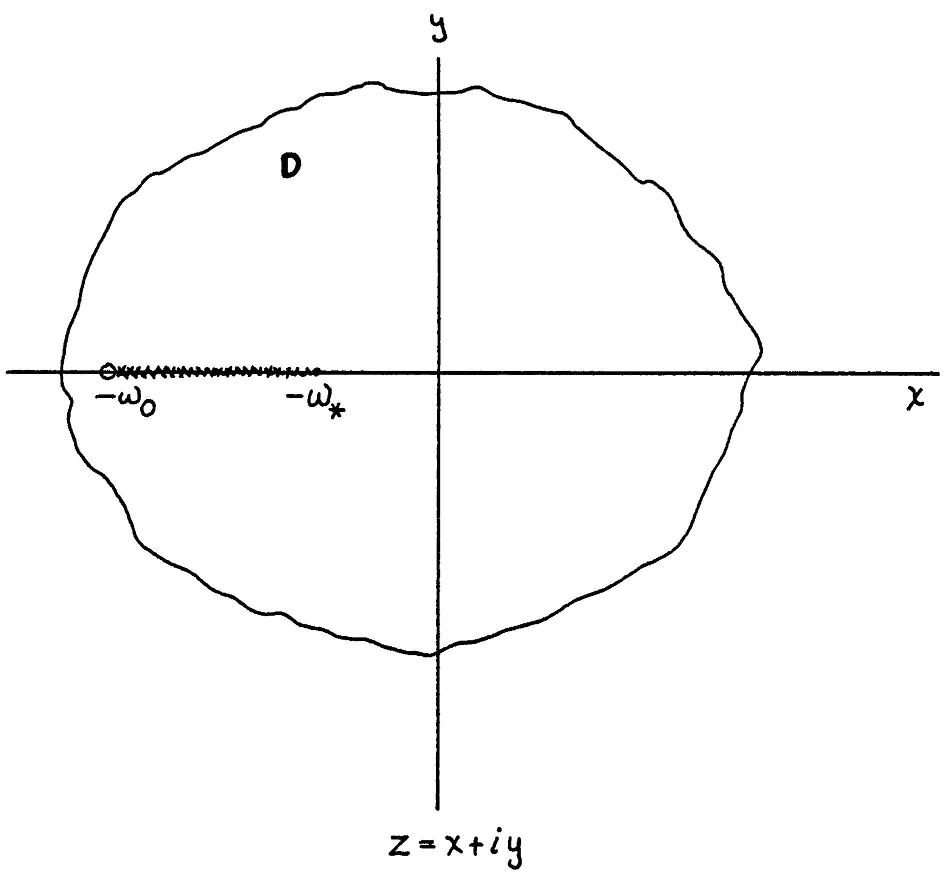

The Domain for the Function g(s) and Its Derivatives

Figure 2.2

Now g(s) and its derivatives are analytic in D, real and well defined for $x \leqq -\omega_0$ and $x > -\omega_*$, and the domain is certainly symmetric about the real axis. Thus,

$$g(\bar{s}) = \overline{g(s)} \qquad 2.8.102$$

and so on.

Define z by

$$z = x + iy, \qquad 2.8.103$$

and then it can be shown that

$$\cosh z = \cosh x \cos y + i \sinh x \sin y, \qquad 2.8.104$$

where the hyperbolic double angle formula and 2.2.35 have been used. From the definition above, it is obvious that

$$\cosh \bar{z} = \overline{\cosh z}. \qquad 2.8.105$$

Section 2.9 Complete Solution to Equation 2.1.29

Data collected during earthquakes are often presented in a form where the motion of the rock underlying sediment deposits is specified, see for example BOGDANOFF, GOLDBERG AND BERNARD[6] or ZEEVAERT[7]. On the assumption that the motion of the bottom of the sediment layer is identical with the motion of the bedrock (or that it can be completely specified if different) and that the surface of a homogeneous layer atop the bedrock is free of tractions, one obtains equation 2.1.29 for the transformed solid displacement. Equation 2.1.29 is inverted by use of the Residue Theorem, and the solution $w_s(x,t)$ is determined in the following sections.

The poles of equation 2.1.29 are $s = \pm i\phi$ and the solutions $(s_{1,2,3})$ of equation 2.2.37.

Since n is never zero, there is one real and one complex conjugate root given by equations 2.5.63 or by the approximations of Section 2.7.

Section 2.10 Steady State Component

In the following, it is convenient to make the following definition

$$F(z) \equiv \frac{\cosh\left[\frac{x}{u_3} g(z)\right]}{\cosh\left[\frac{L}{u_3} g(z)\right]} = a + ib. \qquad 2.10.106$$

The parameters a and b are obtained from equation 2.10.106 by multiplying the numerator and denominator by the conjugate of the denominator, and then separating real and imaginary parts. The result is

$$a = \frac{\cosh x_1 \cos y_1 \cosh x_2 \cos y_2 + \sinh x_1 \sin y_1 \sinh x_2 \sin y_2}{\sinh^2 x_2 + \cos^2 y_2} \qquad 2.10.107$$

and

$$b = \frac{\sinh x_1 \sin y_1 \cosh x_2 \cos y_2 - \cosh x_1 \cos y_1 \sinh x_2 \sin y_2}{\sinh^2 x_2 + \cos^2 y_2}, \qquad 2.10.108$$

where

$$x_1 \equiv \frac{x}{u_3} c(\phi), \quad y_1 \equiv \frac{x}{u_3} d(\phi) \qquad 2.10.109$$

and

$$x_2 \equiv \frac{L}{u_3}\, c(\phi),\; y_2 \equiv \frac{L}{u_3}\, d(\phi). \qquad 2.10.110$$

Also, $g(i\phi)$ is assumed to have been decomposed into real and imaginary parts as

$$g(i\phi) \equiv c(\phi) + id(\phi). \qquad 2.10.111$$

Since the poles at the points $s = \pm i\phi$ are pure imaginary numbers, the function $e^{\pm i\phi t}$ is, by Euler's Formula, periodic and does not decay. Hence, the residues from these poles constitute the steady-state component of the solution.

The residue at $s=-i\phi$ is

Residue =

$$W\phi \lim_{s\to -i\phi}\left\{\frac{(s+i\phi)e^{st}}{(s+i\phi)(s-i\phi)}\; F(s)\right\} = \frac{We^{-i\phi t}}{-2i}\, F(-i\phi). \qquad 2.10.112$$

Similarly, the residue at $s=i\phi$ is

$$\text{Residue} = \frac{We^{i\phi t}}{2i}\, F(i\phi). \qquad 2.10.113$$

Summation of the residues results in the following for the steady-state component

$$\left(\frac{w_s}{W}\right)_{ss} = b\cos\phi t + a\sin\phi t, \qquad 2.10.114$$

where 2.10.106, the Reflection Principle and Euler's Formula have been used.

The functions $c(\phi)$ and $d(\phi)$ are calculated as follows:

$$g(i\phi) = i\phi\left[\frac{\omega_0^2+\phi^2}{\omega_*^2+\phi^2}\right]^{1/4} e^{0.5i(\tan^{-1}\phi/\omega_0-\tan^{-1}\phi/\omega_*)} \qquad 2.10.115$$

where 2.1.27 has been used.

By use of Euler's Formula, $c(\phi)$ and $d(\phi)$ are found to be

$$c(\phi) = -\phi \left[\frac{\omega_0^2+\phi^2}{\omega_*^2+\phi^2}\right]^{1/4} \sin(0.5(\tan^{-1}\phi/\omega_0-\tan^{-1}\phi/\omega_*)) \quad 2.10.116$$

and

$$d(\phi) = \phi \left[\frac{\omega_0^2+\phi^2}{\omega_*^2+\phi^2}\right]^{1/4} \cos(0.5(\tan^{-1}\phi/\omega_0-\tan^{-1}\phi/\omega_*)). \quad 2.10.117$$

When the magnitude of the displacement has a local maximum for some frequency ϕ, this maximum is referred to as a resonance, and the frequency ϕ, as a resonant frequency. Resonances in the steady state occur when

$$\cos\left[\frac{L}{u_3}d(\phi)\right] = 0. \quad 2.10.118$$

Equation 2.10.118 is obtained by manipulating 2.10.114 into the form

$$\left(\frac{w_s}{W}\right)_{ss} = M\sin(\phi t + \alpha), \quad 2.10.119$$

where M is the magnitude and is given by

$$M = \sqrt{a^2 + b^2}. \quad 2.10.120$$

The sinh is not zero for $\phi > 0$, therefore, M is maximized when 2.10.118 vanishes. Equation 2.10.118 is transcendental, and must be solved numerically for the resonant frequencies.

If ϕ/ω_0 and ϕ/ω_* are small compared to 1, then

$$\tan^{-1}\phi/\omega_0 \cong \phi/\omega_0, \quad \tan^{-1}\phi/\omega_* \cong \phi/\omega_*, \quad 2.10.121$$

$$\cos(0.5(\phi/\omega_0 - \phi/\omega_*)) \cong 1 \quad 2.10.122$$

and

$$d(\phi) \cong \phi\sqrt{\frac{\omega_0}{\omega_*}} = \phi\frac{u_3}{u_0} . \qquad 2.10.123$$

Substitution of the approximation for d( ) into equation 2.10.118 gives

$$\cos\left[\frac{L}{u_3}\phi\frac{u_3}{u_0}\right] = 0. \qquad 2.10.124$$

Therefore, the resonant frequencies are approximated by

$$\phi_{res} \cong \frac{2n-1}{2}\frac{\pi}{L}u_0 = \gamma_n u_0, \; n=1,2,... \qquad 2.10.125$$

Note that these resonance frequency approximations are equal to the approximation of the natural frequencies from equation 2.7.90 for $e_n << 1$.

In summary, the steady-state component is

$$\left(\frac{w_s}{W}\right)_{ss} = b\cos\phi t + a\sin\phi t, \qquad 2.10.114$$

where a and b are defined by equations 2.10.107 and 2.10.108.

Section 2.11 The Monotonic-Decaying Component

The component which arises from the residue of the real root s_1 of equation 2.5.63 is computed as follows. Let

$$s_1 \equiv -\xi_n. \qquad 2.11.127$$

The residue is then

Residue =

$$\lim_{s\to-\xi_n}\left\{\frac{W\phi e^{st}\cosh\left[\frac{x}{u_3}g(s)\right]}{s^2+\phi^2}\right\}\lim_{s\to-\xi_n}\left\{\frac{1}{\sinh\left[\frac{L}{u_3}g(s)\right]\frac{L}{u_3}g'(s)}\right\}, \qquad 2.11.128$$

where L'Hospital's Rule has been used on the term in the bracket on the right hand side. By the use of equations 2.2.36, 2.2.30 and 2.2.35, one can calculate, for each value of the index n,

$$\left(\frac{w_s}{W}\right)_{md_n} = \frac{\phi}{\xi_n^2+\phi^2}e^{-\xi_n t}\frac{u_3}{L}\frac{(-1)^{n+1}\cos\left[\frac{x}{L}\pi\frac{2n-1}{2}\right]}{ig'(-\xi_n)}, \qquad 2.11.129$$

$$g'(s) = g(s)\left\{\frac{1}{s}+\frac{1}{2}\frac{\omega_*-\omega_0}{(s+\omega_0)(s+\omega_*)}\right\}. \qquad 2.11.130$$

and

$$g'(-\xi_n) = -i\,\frac{2n-1}{2}\pi\frac{u_3}{L}\left\{\frac{-1}{\xi_n}+\frac{1}{2}\frac{\omega_*-\omega_0}{(\omega_0-\xi_n)(\omega_*-\xi_n)}\right\}. \qquad 2.11.131$$

Summation of all the terms of 2.11.129 over n, and factoring out a g(s) in the denominator gives

$$\left(\frac{w_s}{W}\right)_{md} = \sum_{n=1}^{\infty}\left\{\frac{2(-1)^{n+1}}{(2n-1)\pi}\frac{\phi}{\xi_n^2+\phi^2}\frac{e^{-\xi_n t}\cos\left[\frac{x}{L}\pi\frac{2n-1}{2}\right]}{\left\{\frac{-1}{\xi_n}+\frac{1}{2}\frac{\omega_*-\omega_0}{(\omega_0-\xi_n)(\omega_*-\xi_n)}\right\}}\right\}. \qquad 2.11.132$$

The term $(\omega_0-\xi_n)$, which appears as a divisor, is likely to be zero when calculated by use of finite precision arithmetic until n becomes quite large, as may be seen by inspection of equation 2.7.92. To prevent division by zero, the approximation 2.7.92 for s_1 should be used when $e_n \ll 1$.

Section 2.12 Cyclic-Decaying Component

The final component is that due to the residue of the complex conjugate root, s_2 and s_3. Let

$$s_{2,3} \equiv -\zeta_n \pm i\omega_n, \qquad 2.12.133$$

and the cyclic-decaying component is given, for each n, by the sum of the residue due to $s=s_2$

Residue =

$$\lim_{s\to s_2}\left\{\frac{\phi e^{st}\cosh\left[\frac{x}{u_3}g(s)\right]}{s^2+\phi^2}\right\}\lim_{s\to s_2}\left\{\frac{s-s_2}{\cosh\left[\frac{L}{u_3}g(s)\right]}\right\}, \qquad 2.12.134$$

and the residue due to $s=s_3$ (which will be the conjugate of 2.12.134). The term in the left hand side bracket of 2.12.134 (for $s=s_2$) when evaluated is

$$\lim_{s\to s_2}\left\{\frac{\phi e^{st}\cosh\left[\frac{x}{u_3}g(s)\right]}{s^2+\phi^2}\right\} =$$

$$e^{-\zeta_n t}e^{i\omega_n t}\frac{\phi}{(-\zeta_n+i\omega_n)^2+\phi^2}\cos\left[\frac{x}{L}\pi\frac{2n-1}{2}\right]. \qquad 2.12.135$$

When $s=s_3$, the result is the conjugate of 2.12.135 since $s^2+\phi^2$ also obeys the conditions required by the Reflection Principle. For convenience, the following definition is made

$$G_n \equiv (-\zeta_n + i\omega_n)^2 + \phi^2 = C_n + iD_n. \qquad 2.12.136$$

By use of L'Hospital's Rule, the term in the right hand side bracket of 2.12.134 is

$$\lim_{s \to s_2} \left\{ \frac{s-s_2}{\cosh\left[\frac{L}{u_3} g(s)\right]} \right\} = \lim_{s \to s_2} \left\{ \frac{1}{\frac{L}{u_3} g'(s) \sinh\left[\frac{L}{u_3} g(s)\right]} \right\}, \qquad 2.12.137$$

where

$$\sinh\left[\frac{L}{u_3} g(s)\right] = \sinh\left[\pm i\pi \frac{2n-1}{2}\right] = \pm(-1)^{n+1}, \qquad 2.12.138$$

and

$$g'(s_2) = \pm i\pi \frac{2n-1}{2} \quad \frac{u_3}{L} \left\{ \frac{1}{s_2} + \frac{1}{2} \frac{\omega_* - \omega_0}{(s_2+\omega_0)(s_2+\omega_*)} \right\}. \qquad 2.12.139$$

Given the following definition

$$F_n \equiv \frac{1}{-\zeta_n + i\omega_n} + \frac{1}{2} \frac{\omega_* - \omega_0}{(-\zeta_n + i\omega_n + \omega_0)(-\zeta_n + i\omega_n + \omega_*)} = A_n + iB_n, \qquad 2.12.140$$

the cyclic-decaying component for each n can be written as

$$\left(\frac{w_s}{W}\right)_{cd_n} = \frac{2\phi e^{-\zeta_n t} (-1)^n \cos\left[\frac{x}{L}\pi \frac{2n-1}{2}\right]}{(2n-1)\pi} \left\{ \frac{e^{i\omega_n t}}{G_n F_n} + \frac{e^{-i\omega_n t}}{\overline{G}_n \overline{F}_n} \right\}. \qquad 2.12.141$$

The term $(GF)_n^{-1}$ is given by,

$$\frac{1}{G_n F_n} = \frac{(A_n C_n - B_n D_n) - i(D_n A_n + B_n C_n)}{(A_n C_n - B_n D_n)^2 + (D_n A_n + B_n C_n)^2} = a_n' - ib_n', \qquad 2.12.142$$

where equations 2.12.140 and 2.12.136 have been used.

Now finally, with the use of Euler's Formula, the bracketed term in equation 2.12.141 is found to be

$$\frac{e^{i\omega_n t}}{G_n F_n} + \frac{e^{-i\omega_n t}}{\overline{G}_n \overline{F}_n} = 2a_n' \cos\omega_n t + 2b_n' \sin\omega_n t. \qquad 2.12.143$$

Summation of 2.12.141 over n gives the cyclic-decaying term

$$\left(\frac{w_s}{W}\right)_{cd} = \sum_{n=1}^{\infty} \left\{ \frac{4\phi e^{-\zeta_n t}(-1)^n}{(2n-1)\pi} \cos\left[\frac{x}{L}\pi\frac{2n-1}{2}\right] (a_n' \cos\omega_n t + b_n' \sin\omega_n t) \right\}, \qquad 2.12.144$$

where

$$a_n' = \frac{(A_n C_n - B_n D_n)}{(A_n C_n - B_n D_n)^2 + (D_n A_n + B_n C_n)^2}, \qquad 2.12.145$$

$$b_n' = \frac{(D_n A_n + B_n C_n)}{(A_n C_n - B_n D_n)^2 + (D_n A_n + B_n C_n)^2}, \qquad 2.12.146$$

$$C_n = (\phi^2 - \omega_n^2) + \zeta_n^2, \qquad 2.12.147$$

$$D_n = -2\omega_n \zeta_n, \qquad 2.12.148$$

$$A_n = \frac{-\zeta_n}{\zeta_n^2 + \omega_n^2} + \frac{0.5(\omega_* - \omega_0)((\omega_0 - \zeta_n)(\omega_* - \zeta_n) - \omega_n^2)}{((\omega_0 - \zeta_n)^2 + \omega_n^2)((\omega_* - \zeta_n)^2 + \omega_n^2)} \qquad 2.12.149$$

and

$$B_n = \frac{-\omega_n}{\zeta_n^2 + \omega_n^2} - \frac{0.5(\omega_* - \omega_0)\omega_n(\omega_0 + \omega_* - 2\zeta_n)}{((\omega_0 - \zeta_n)^2 + \omega_n^2)((\omega_* - \zeta_n)^2 + \omega_n^2)}. \qquad 2.12.150$$

Section 2.13 Total Response

The total solid displacement is the superposition of the three components

$$\left(\frac{w_s}{W}\right) = \left(\frac{w_s}{W}\right)_{ss} + \left(\frac{w_s}{W}\right)_{md} + \left(\frac{w_s}{W}\right)_{cd} \qquad 2.13.151$$

given by equations 2.10.114,2.11.132 and 2.12.144.

This solution is evaluated numerically for two materials and the results are given in the next chapter.

CHAPTER III

NUMERICAL RESULTS

Introduction

Numerical results serve at least two purposes: i. exposing heretofore unnoticed errors in deriving a particular solution and ii. establishing the importance of various effects present in the solution. Thus if for instance, fluid viscosity terms are added to a model and the numbers flowing out of the computer do not change, then viscosity effects are probably not important enough to worry about. With this observation as a prelude, the present chapter examines the relative importance of including inertial terms in the model described in Chapter I.

It is sometimes difficult to make the transition from an analytic formulation of a solution to a computer program to evaluate the solution. The main reason for this difficulty is that arithmetic on a computer is carried out with finite precision. So, for example, arithmetic is not necessarily associative, and the order in which the terms are evaluated makes a big difference. The form of the solution in Chapter II reflects the ordering of terms found to be acceptable to the computer.

A listing of the FORTRAN IV program used to evaluate the solution and print out maximum displacements may be found in the appendix. A list of computer notation and a list of the subroutines used follows in the next two sections.

Section 3.1 List of Computer Notation

Variable Name	Description	Text Symbol	Equation
XID	DRAG COEFFICIENT	ξ	1.3.13
OMEGA0	CHAR. FREQ.	ω_0	1.2.11
OMEGA1	CHAR. FREQ.	ω_*	2.1.27
U1	ACCEL. WAVE SPEED	u_3	1.2.9
U0	FROZ. WAVE SPEED	u_0	1.2.10
SRU1U0	RATIO OF ABOVE		
RHOF	FLUID BULK DENS.	ρ_f	1.1.6
RHOS	SOLID BULK DENS.	ρ_s	1.1.7
PHIF	POROSITY	ϕ_f	1.3.13
GAMMAF	TRUE FLUID DENS.	γ_f	
GAMMAS	TRUE SOLID DENS.	γ_s	
MUS	SHEAR MODULUS	μ_s	1.1.7
GAMMAN	1/LENGTH USED FOR CALCULATING POLES	γ_n	2.2.36
XIN	|REAL ROOT|	ξ_n	2.11.127
ZETAN	|REAL PART OF COMP. CONJ. ROOT|	ζ_n	2.12.133
OMEGAN	|IMAG. PART OF COMP. CONJ. ROOT|	ω_n	2.12.133
PHIR	RES. FREQ. OF WSS	ϕ_{res}	2.10.125
L	DEPTH OF FORMATION	L	1.4.21
X	POSITION IN FORM.	x	1.1.7
N	INDEX	n	2.10.125
C	REAL PART OF g(s)	$c(\phi)$	2.10.111
D	IMAG. PART OF g(s)	$d(\phi)$	2.10.111
MCDA,B	MAGNITUDES OF WCD		

Variable Name	Description	Text Symbol	Equation
MMD	MAGNITUDE OF WMD		
MSA,B	MAGNITUDES OF WSS		
NUMPHI	NUM. OF RESONANCES OF SS AND CD COMP		
NUMCYC	NUMBER OF CYCLES		
PI		π	
DT	TIME STEP		
T	TIME	t	
WSS	STEADY-STATE COMP.	$()_{ss}$	2.10.114
WMD	MONOTONIC-DECAYING COMPONENT	$()_{md}$	2.11.132
WCD	CYCLIC-DECAYING COMPONENT	$()_{cd}$	2.12.145
WS	TOTAL RESPONSE	w_s	2.13.151
DMAX	MAXIMUM TIME SERIES OF WS		
DSSMAX	MAXIMUM WSS VALUE		
RMSMAX	ROOT MEAN SQUARE OF SS TERM AND ALL SIG. TERMS OF WMD AND WCD.		
TMAX	TIME AT WHICH DMAX OCCURS		
PHICYC	DUMMY		
CYC	DUMMY		
PART1,	" "		
DUM, ETC	DUMMY		
PHI	FREQ. APPLIED TO THE BOUNDARY	ϕ	1.4.21

Section 3.2 List of Subroutines

INPUT Reads in the material parameters from a disk file.

PROP Calculates the necessary quantities from those read in through INPUT.

PRINTP Prints out the values read in and the ones calculated by PROP.

ROOTS Calculates the values XIN, ZETAN and OMEGAN which are the components of the poles.

PHIRES Calculates a resonant frequency of the steady-state component.

CDPHI Computes the functions $c(\phi)$ and $d(\phi)$.

CALMCD Calculates the time invariant part of the non-dimensional magnitudes (a'and b') of the cyclic-decaying component.

CALMMD Calculates the time invariant part of the non-dimensional magnitude of the monotonic-decaying component.

SSCOMP Calculates the non-dimensional magnitude (a and b) of the steady-state component.

DISPM Adds the time dependence to the various magnitudes and calculates the sinusoidal terms. Calculates the total response and stores the time series maximum over a specified range with a specified number of time divisions. Calculates the root mean square of all the magnitudes (time dependent), stores the maximum, and calculates the magnitude of the steady-state.

CALPHI Returns a vector PHIRS with the first NUMPHI natural frequencies and then the first NUMPHI steady-state frequencies.

Section 3.3 Flow Chart for Program RESO

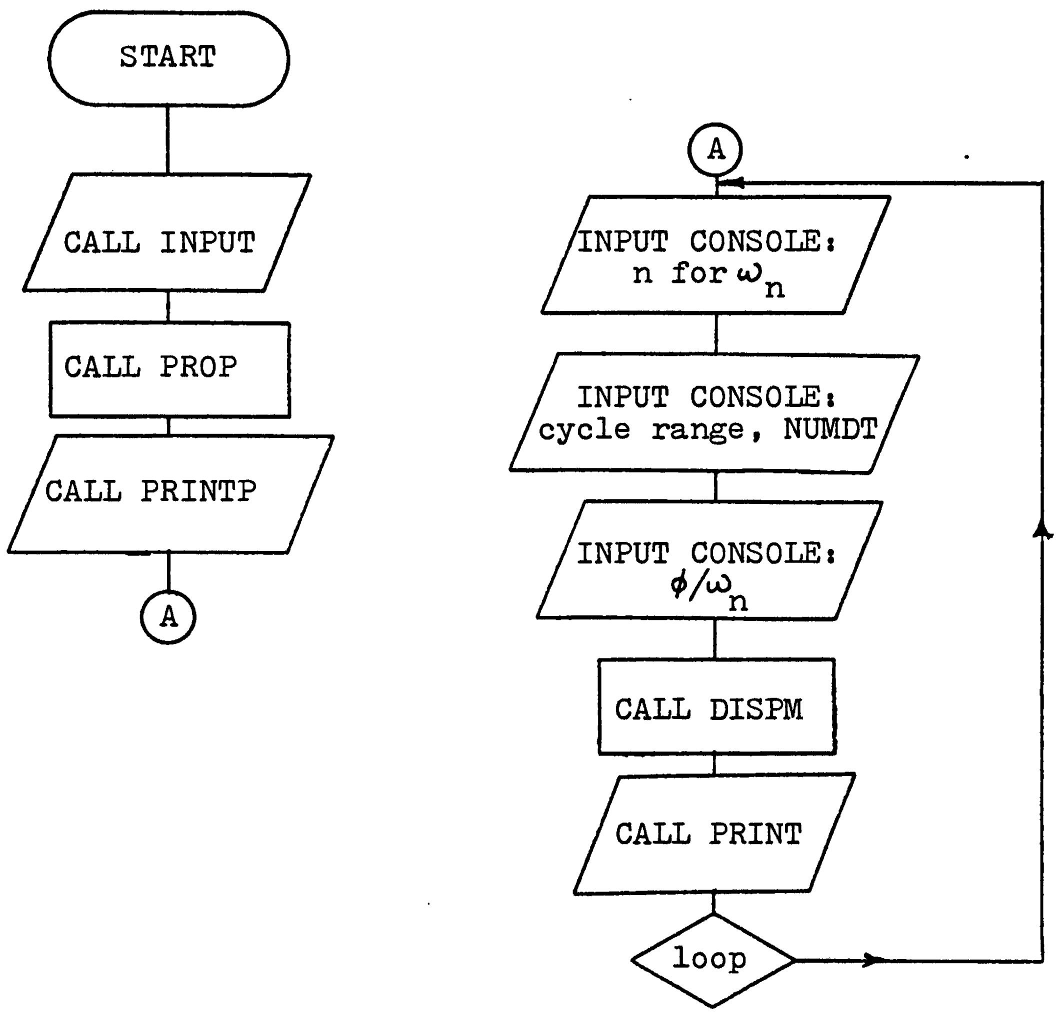

Section 3.4 Displacement Spectra

The almost ceaseless spewing forth of data that computers are capable of has been distilled here into displacement spectra. These graphs relate the maximum displacement which occurs in the formation, at a certain value of x for all time, to the forcing frequency applied on the boundary. Of course, important information is left out by the use of displacement spectra. For example, the time the maximum occurs is not available. Also there is no indication of the how large the displacements were which preceded the maximum. The time at which the maximum occurs is shown for five input frequencies in figures 3.2 and 3.5. Here, the purpose is to demonstrate the importance of the inertial terms, and the spectra are ideal for this purpose since any dependence on the forcing frequency is a consequence of including their effects. Also, spectra are typically used by engineers for design purposes, and the time a maximum occurs is usually less important than the numerical value of the maximum displacement.

There are three estimates of the maximum which are calculated by RESO:

i. Time Series Estimate (DMAX). The output is sampled at discrete points as time goes on, keeping the maximum.

ii. Steady-State Maximum (DSSMAX). The magnitude of the steady-state component is computed so that the relative effect of the transient components may be calculated.

iii. Root Mean Square (RMSMAX). The square root of the sum of the squares of all the terms used in computing DMAX, apart from the sinusoidal terms, is computed. In the materials considered, the natural frequencies are relatively high so that many cycles occur within the 180 second search limit. In this case, the maximum is very near the sum of the absolute magnitudes, which can be estimated by multiplying RMSMAX by the square root of 2 . This gives DSMAX to such accuracy that DSMAX could be omitted if the time at which it occurs is not important.

For the materials considered, the cyclic-decaying component decays very slowly, as may be inferred from the magnitude of ZETAN given in the next two sub-sections. The monotonic-decaying component on the other hand barely exists at all. Besides having, for the material used, a very small magnitude, it decays extremely rapidly in time, as is indicated by the magnitude of XIN.

Spectra are presented for two materials, Berea Sandstone and Ruhr Sandstone, the properties of which are taken from the table given in RICE AND CLEARY[2] and the densities are taken from FARMER[10]. The points plotted were obtained interactively using the program RESO. Intelligence is difficult to encode in a program, and it was easier to leave the decision, with regard to whether a maximum had been reached and when, to the operator. A value was chosen as a maximum if over the next two cycles of the nearest fundamental frequency (ω_n), the value was not exceeded. Usually in about a half to two thirds the time it took to reach maximum, values as high as 80-90% of maximum had occured.

Section 3.4.1 Berea Sandstone

In this sub-section, results for Berea Sandstone are presented. First, there is output from the program RESO showing the input to the program and some important values calculated from the input. The decay exponents and natural and steady-state resonant frequencies are also shown. Second, there is a bar graph showing the peaks in the spectra at 99.9% of the first five natural frequencies and the times at which they occur. A cut off time of 180 seconds was applied, this is about the duration of the larger earthquakes. The peak of the spectra is very sharply pointed, and the evaluation of the solution itself shows some problems because of finite precision truncation. Near the peak though, the solution still converges to the initial conditions and is well behaved. Third, a plot of the displacement spectrum is given where the actual values of DMAX calculated are marked with X's, and the solid line is $\sqrt{2}$ *RMSMAX.

PROGRAM RESO BEREA SANDSTONE

MATERIAL PROPERTIES

INPUT		
POSITION IN FORMATION	5000.000	CM
FORMATION DEPTH	10000.000	CM
TRUE DENSITY, FLUID	1.000	G/CC
BULK DENSITY, SOLID	2.600	G/CC
SHEAR MODULUS, SOLID	.6000000E+11	DYNES/SQ-CM
POROSITY	.1900000	VOL/VOL
PERMIABILITY	.1900000E-08	SQ-CM
VISCOSITY, FLUID	.9800000E-02	POISE
OUTPUT		
DRAG COEFFICIENT	.1862000E+06	DYNE-SEC/CM**4
ACCELERATION WAVE SPEED	.1519109E+06	CM/SEC
FROZEN WAVE SPEED	.1466471E+06	CM/SEC
RATIO OF ACCEL BY FROZEN, SQUARED	1.0730770	
RECIPROCAL CHAR. TIME FOR DIFF.	.1051615E+07	RAD/SEC

Table 3.1 Berea Sandstone: Material Properties, Decay Exponents and Resonant Frequencies

OUTPUT OF DECAY EXPONENTS AND NATURAL FREQUENCIES

N	MONOTONIC-DECAYING EXPONENT XIN	CYCLIC-DECAYING EXPONENT ZETAN	CYCLIC-DECAYING NATURAL FREQ. OMEGAN	STEADY-STATE RESONANCE FREQ. PHIR
1	.1051615E+07	.1843655E-04	23.03526	23.03528
2	.1051615E+07	.1659289E-03	69.10577	69.10582
3	.1051615E+07	.4609139E-03	115.17628	115.17638
4	.1051615E+07	.9033913E-03	161.24680	161.24693
5	.1051615E+07	.1493359E-02	207.31731	207.31749
6	.1051615E+07	.2230825E-02	253.38782	253.38803
7	.1051615E+07	.3115781E-02	299.45834	300.73672
8	.1051615E+07	.4148226E-02	345.52884	345.52908
9	.1051615E+07	.5328164E-02	391.59937	391.59970
10	.1051615E+07	.6655604E-02	437.66989	437.67017
11	.1051615E+07	.8130521E-02	483.74039	483.74069
12	.1051615E+07	.9752944E-02	529.81091	529.81128
13	.1051615E+07	.1152286E-01	575.88141	575.88184
14	.1051615E+07	.1344027E-01	621.95197	623.23077
15	.1051615E+07	.1550516E-01	668.02246	667.74713
16	.1051615E+07	.1771753E-01	714.09296	714.09357
17	.1051615E+07	.2007741E-01	760.16345	760.16425
18	.1051615E+07	.2258480E-01	806.23395	806.23474
19	.1051615E+07	.2523965E-01	852.30450	852.30542
20	.1051615E+07	.2804202E-01	898.37500	898.37585

Table 3.1 Continued

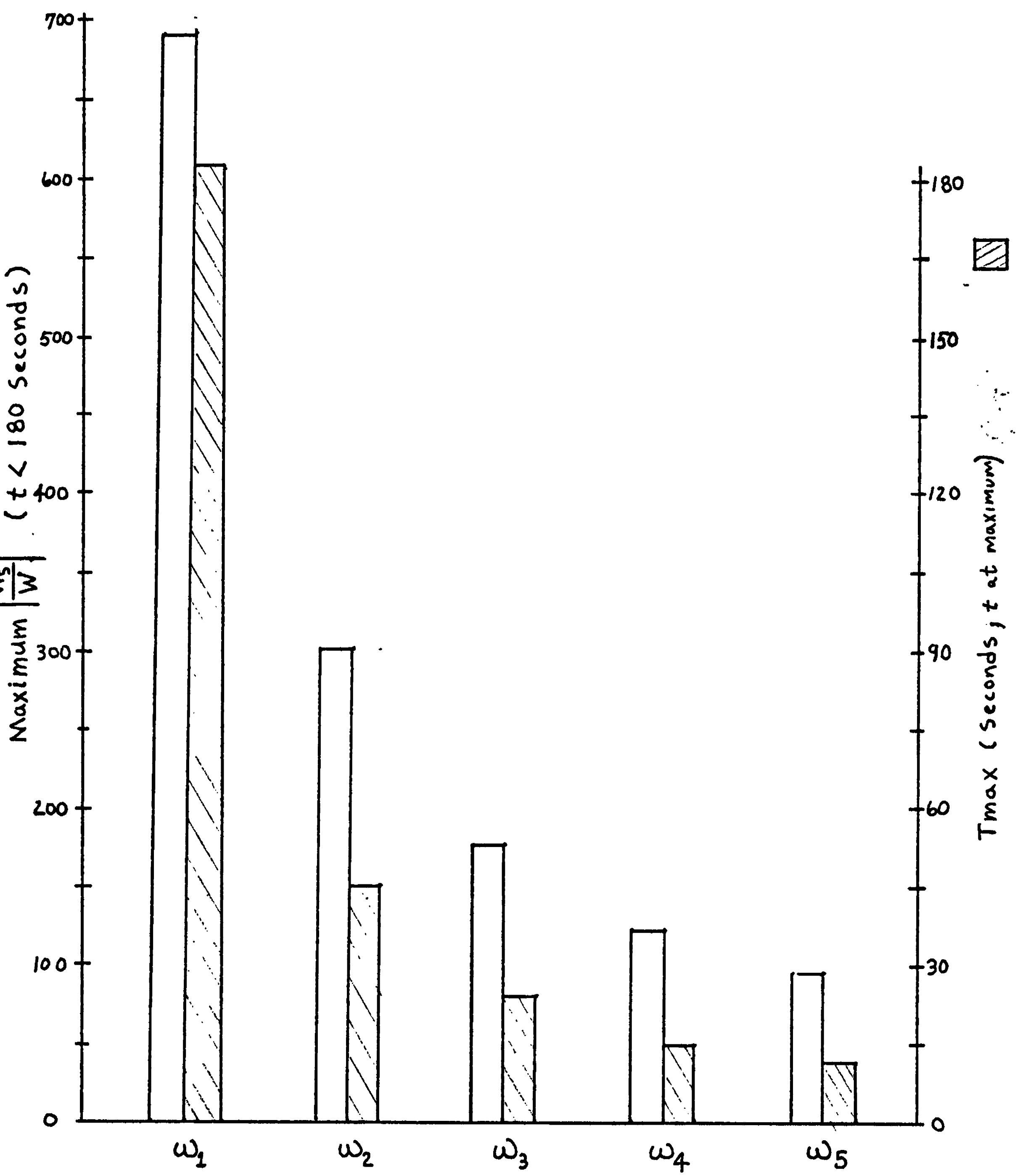

Figure 3.2 Berea Sandstone: Maximum Displacement and T_{max} at $\phi = .999\,\omega_n$

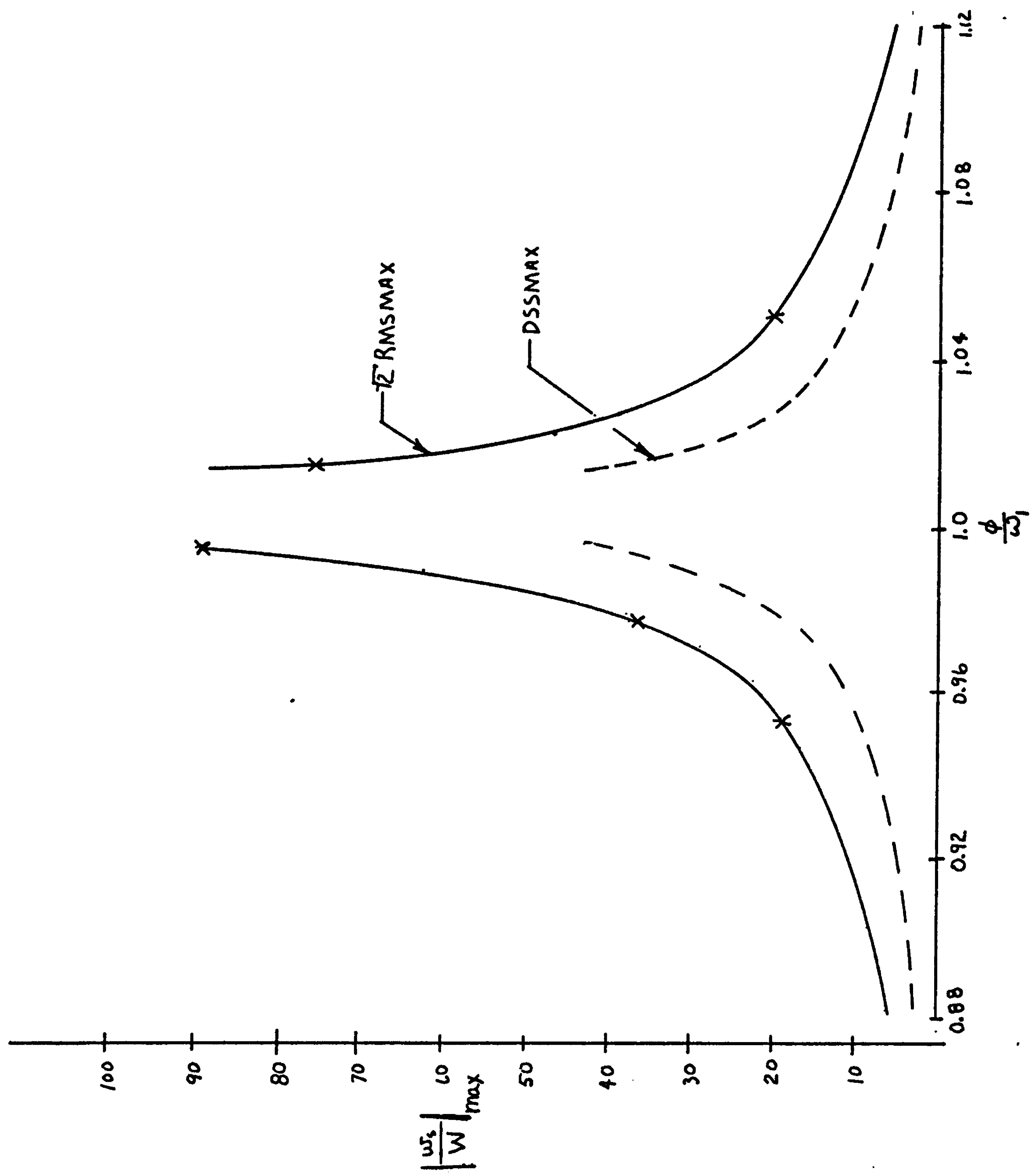

Figure 3.3 Berea Sandstone: Displacement Spectra
Near $\phi = \omega_1$

Section 3.4.2 Ruhr Sandstone

In this sub-section, results for Ruhr Sandstone are presented. First, there is output from the program RESO showing the input to the program and some important values calculated from the input. The decay exponents and natural and steady-state resonant frequencies are also shown. Second, there is a bar graph showing the peaks in the spectra at 99.9% of the first five natural frequencies and the times at which they occur. A cut off time of 180 seconds was applied, this is about the duration of the larger earthquakes. The peak of the spectra is very sharply pointed, and the evaluation of the solution itself shows some problems because of finite precision truncation. Near the peak though, the solution still converges to the initial conditions and is well behaved. Third, a plot of the displacement spectrum is given where the actual values of DMAX calculated are marked with X's, and the solid line is $\sqrt{2}$ *RMSMAX.

PROGRAM RESO RUHR SANDSTONE		
MATERIAL PROPERTIES		
INPUT		
POSITION IN FORMATION	5000.000	CM
FORMATION DEPTH	10000.000	CM
TRUE DENSITY, FLUID	1.000	G/CC
BULK DENSITY, SOLID	2.600	G/CC
SHEAR MODULUS, SOLID	.1330000E+12	DYNES/SQ-CM
POROSITY	.0200000	VOL/VOL
PERMIABILITY	.2000000E-11	SQ-CM
VISCOSITY, FLUID	.9800000E-02	POISE
OUTPUT		
DRAG COEFFICIENT	.1960000E+07	DYNE-SEC/CM**4
ACCELERATION WAVE SPEED	.2261722E+06	CM/SEC
FROZEN WAVE SPEED	.2253073E+06	CM/SEC
RATIO OF ACCEL BY FROZEN, SQUARED	1.0076923	
RECIPROCAL CHAR. TIME FOR DIFF.	.9875385E+08	RAD/SEC

Table 3.4 Ruhr Sandstone: Material Properties, Decay Exponents and Resonant Frequencies

OUTPUT OF DECAY EXPONENTS AND NATURAL FREQUENCIES

N	MONOTONIC-DECAYING EXPONENT XIN	CYCLIC-DECAYING EXPONENT ZETAN	CYCLIC-DECAYING NATURAL FREQ. OMEGAN	STEADY-STATE RESONANCE FREQ. PHIR
1	.9875385E+08	.4878211E-07	35.39116	35.39118
2	.9875385E+08	.4390349E-06	106.17345	106.17353
3	.9875385E+08	.1219543E-05	176.95576	176.95590
4	.9875385E+08	.2390288E-05	247.73807	247.73824
5	.9875385E+08	.3951387E-05	318.52036	318.52060
6	.9875385E+08	.5902606E-05	389.30264	389.30292
7	.9875385E+08	.8244147E-05	460.08499	462.04904
8	.9875385E+08	.1097607E-04	530.86731	530.86761
9	.9875385E+08	.1409805E-04	601.64960	601.65002
10	.9875385E+08	.1761046E-04	672.43188	672.43237
11	.9875385E+08	.2151300E-04	743.21417	743.21472
12	.9875385E+08	.2580564E-04	813.99652	813.99707
13	.9875385E+08	.3048871E-04	884.77881	884.77924
14	.9875385E+08	.3556209E-04	955.56116	957.52551
15	.9875385E+08	.4102539E-04	1026.34338	1025.92029
16	.9875385E+08	.4687969E-04	1097.12573	1097.12646
17	.9875385E+08	.5312374E-04	1167.90796	1167.90881
18	.9875385E+08	.5975971E-04	1238.69019	1238.69116
19	.9875385E+08	.6678205E-04	1309.47266	1309.47351
20	.9875385E+08	.7419754E-04	1380.25488	1380.25586

Table 3.4 Continued

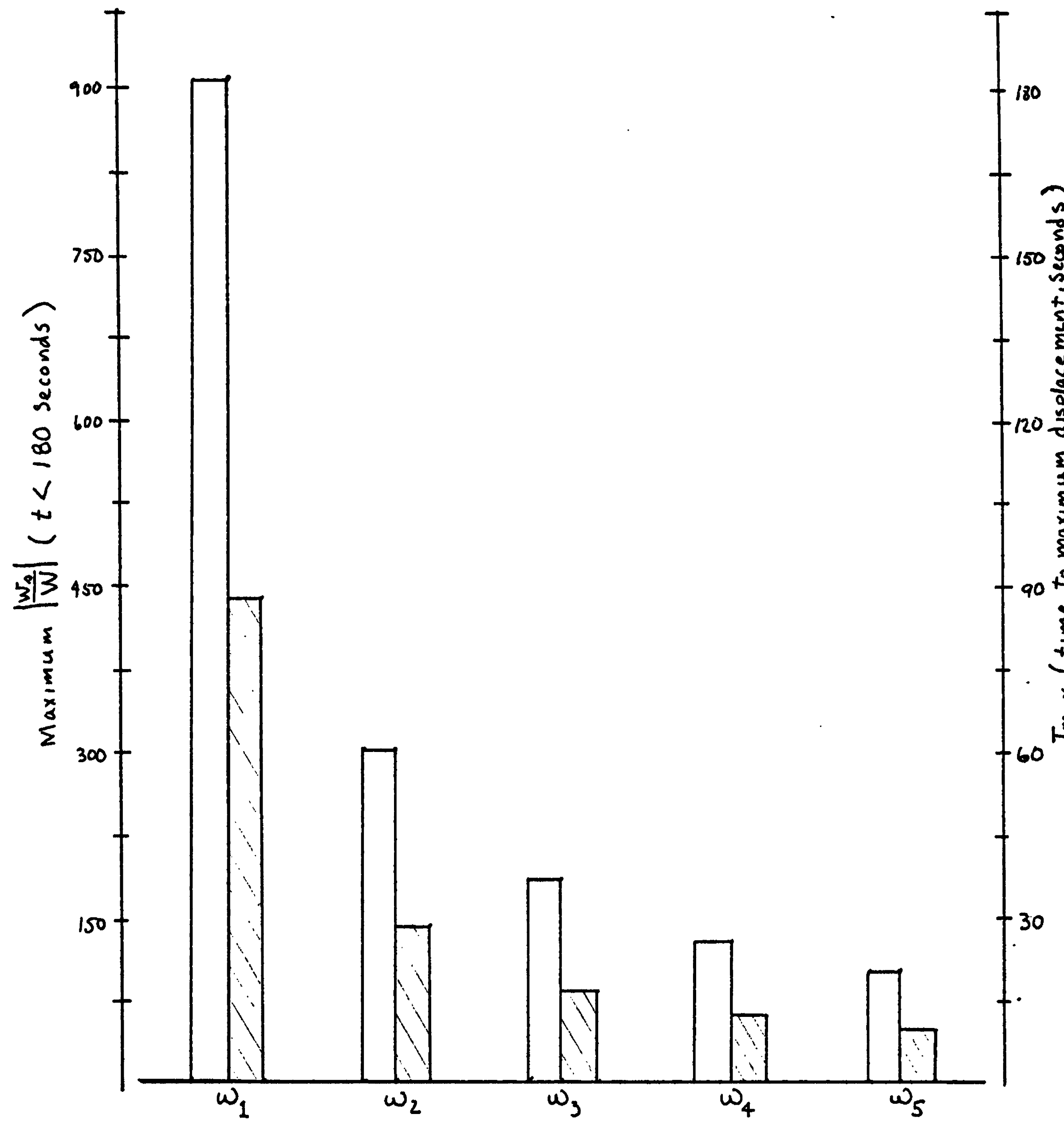

Figure 3.5 Ruhr Sandstone: Maximum Displacement and T_{max} at ϕ =.999 ω_n

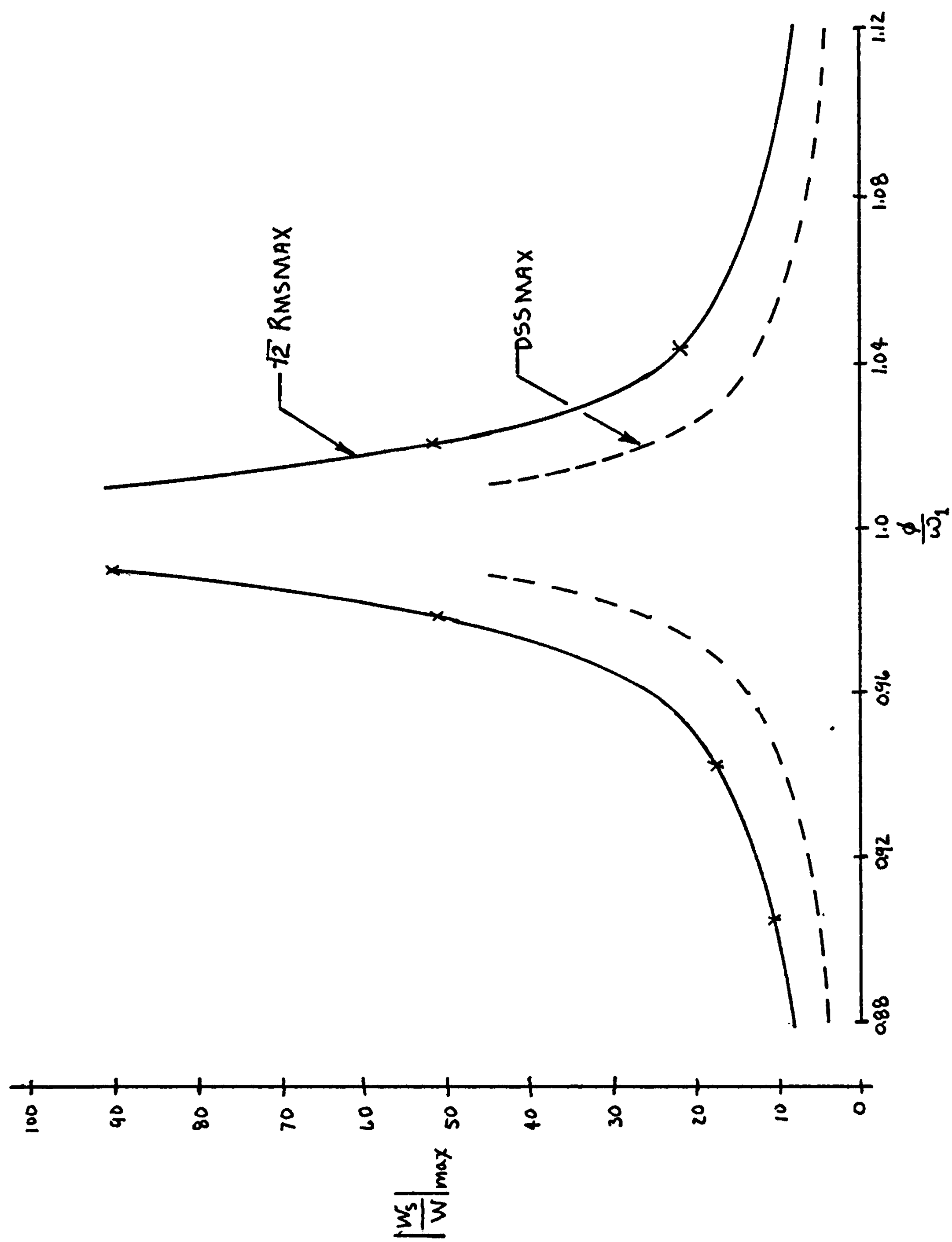

Figure 3.6 Ruhr Sandstone: Displacement Spectra
Near $\phi = \omega_1$

Section 3.5 Conclusions

An analytic solution for shear motions in a binary mixture of a chemically inert, isothermal, elastic isotropic solid and elastic fluid subject to a sinusoidally varying solid displacement on one boundary and traction free on the other was obtained. This solution was evaluated with the aid of a computer program for two materials. The results were plotted in the form of displacement spectra. Resonances or peaks in these spectra were found indicating the influence of inertial terms. Enhancement on the order of hundreds of times the exciting displacement was found near the resonant frequencies. Significant enhancement also extended to either side of the peak for a range of 10-20% of the normalized frequency (ϕ/ω_n). Depending on the geometry, material, or location in the formation, the enhancements could be larger still.

The conclusion is that inertial effects are very important when studying the effects of time varying boundary conditions on porous media, and may not be neglected as is commonly done.

BIBLIOGRAPHY

1. Bowen, R.M., Theory of Mixtures in Continuum Physics, Vol. III, Erigen, A.C., ed., Academic Press, NY,1976.

2. Rice, J.R. and Cleary, M.P., Some Basic Stress Diffusion Solutions for Fluid-Saturated Elastic Porous Media with Compressible Constituents, Reviews of Geophysics and Space Physics, Vol. 14, 227-241,1976.

3. Biot, M.A., General Theory of Three Dimensional Consolidation, J. Appl. Phys., Vol. 12, 155-164, 1941.

4. Uspensky, J.V., Theory of Equations, Mc-Graw-Hill Book Co.,NY,1948.

5. Schneider, W.C., A Study of Linear Fluid-Solid Mixtures, Ph.D. Thesis, Rice University, 1972.

6. Bogdanoff, J.L., Goldberg, J.E. and Bernard, M.C., Response of a Simple Structure to a Random Earthquake-Type Disturbance, Bul. of the Seismological Soc. of Am., Vol. 51, No. 2, 293-310., April, 1961.

7. Zeevaert, L., Foundation Engineering for Difficult Subsoil Conditions, Van Nostrand Reinhold, NY, 1973.

8. Churchill, R.V., Modern Operational Mathematics in Engineering, Mc Graw-Hill Book Co., NY, 1944.

9. Churchill, R.V., Brown, J.W., Verhey, R.F., Complex

Variables and Applications, 3rd. ed., Mc Graw-Hill Book Co., NY, 1976.

10. Farmer, I.W., Engineering Properties of Rocks, E. and F.N. Spon Ltd., London, p15, 1968.

11. Hovanessian, S.A., Pipes, L.A., Digital Computer Methods in Engineering, Mc Graw-Hill Book Co., NY, 1969.

APPENDIX

LISTING OF PROGRAM RESO

```
      PROGRAM RESO
      DIMENSION PHIRS(20)
      REAL MUW,MUS,L,K,NUMCYC
C LUN=5 IS THE CONSOLE
C LUN=6 IS A DISK DRIVE
C LUN=2 IS THE PRINTER
      CALL INPUT(PHIF,GAMMAF,GAMMAS,MUS,K,MUW,X,L,
     *NUMPHI,NUMDT,NDUM)
      NUMCYC=FLOAT(NDUM)
C     CALL DSKOFF
      JKDUM=0
      IF(JKDUM.NE.0) GOTO 999
      CALL PROP(PHIF,GAMMAF,GAMMAS,MUS,K,MUW,XID,U1
     *,U0,SRU1U0,OMEGA0,OMEGA1)
      CALL PRINTP(PHIF,GAMMAF,GAMMAS,MUS,K,MUW,XID,U1
     *,U0,SRU1U0,OMEGA0,OMEGA1,X,L)
              DO 88 LDUM=1,20
                CALL PHIRES(OMEGA0,OMEGA1,U0,L,LDUM,PHIR)
                GAMMAN=3.14159*FLOAT(2*LDUM-1)/2./L
                CALL ROOTS(OMEGA0,U1,U0,GAMMAN,XIN,ZETAN,OMEGAN)
                WRITE(7,87) LDUM,XIN,ZETAN,OMEGAN,PHIR
87              FORMAT(I7,2E20.7,2F20.5)
88            CONTINUE
      CALL CALPHI(OMEGA0,OMEGA1,U1,U0,L,NUMPHI,PHIRS)
      DUMCYC=0.
11    WRITE(5,2) JK
2     FORMAT(1X,'RESONANCE FREQ. INDEX= ',I7/)
      READ(5,1) JK
1     FORMAT(I7)
      WRITE(5,22) DUMCYC,NUMCYC,NUMDT
      READ(5,23) NTEST
22    FORMAT(1X,'DUMCYC= ',F15.5,'  NUMCYC= ',F15.5,' NUMDT= ',I7/
     *1X,'CHANGE VALUES? YES=1, NO=0'/)
23    FORMAT(I2)
      IF(NTEST.EQ.0) GOTO 27
      READ(5,24) DUMCYC,NUMCYC,NUMDT
```

```
24      FORMAT(2F15.5,I7)
27      WRITE(5,28)
28      FORMAT(1X,'ENTER FREQ. DIVIDED BY OMEGA1'/)
        READ(5,29) RPO
29      FORMAT(F15.5)
        CYC=NUMCYC
        OMEGA=PHIRS(JK)*RPO
        I=0
        DUMO=AMIN1(OMEGA,PHIRS(JK))
        CALL DISPM(OMEGA,OMEGA0,OMEGA1,U1,U0,SRU1U0,
     *L,X,NUMPHI,NUMDT,CYC,DUMCYC,DUMO,DMAX,DSSMAX,RMSMAX,TMAX)
        CALL PRINT(I,OMEGA,RPO,DMAX,DSSMAX,RMSMAX,TMAX)
        GOTO 11
999     STOP
        END
C
C
        SUBROUTINE PRINT(I,PHI,RATIO,DMAX,DSSMAX,RMSMAX,TMAX)
        WRITE(5,10) I,PHI,RATIO
        WRITE(5,20) DMAX,TMAX,DSSMAX,RMSMAX
10      FORMAT(//6X,'FREQUENCY NUMBER  ',9X,I7/
     *6X,'FREQENCY  ',9X,8X,F15.5,'  RAD/SEC'/
     *6X,'FREQ. MULT. BY CHAR. TIME  ',F15.5/)
20      FORMAT(6X,'MAXIMUM TIME SERIES DISP.  ',F15.5,'  CM/CM'/
     *6X,'TIME AT MAX  ',14X,F15.5,'  SEC'/
     *6X,'MAXIMUM STEADY-STATE DISP. ',F15.5,'  CM/CM'/
     *6X,'MAXIMUM RMS VALUE  ',8X,F15.5,'  CM/CM'/)
        RETURN
        END
C
C
        SUBROUTINE INPUT(PHIF,GAMMAF,GAMMAS,MUS,K,MUW,X,L,
     *NUMPHI,NUMDT,NUMCYC)
        REAL MUS,MUW,L,K
        CALL OPEN(6,'RESO    DAT',0)
        READ(6,10) PHIF,K,MUW
```

```
      READ(6,20) GAMMAF,GAMMAS,MUS
      READ(6,30) X,L
      READ(6,40) NUMPHI,NUMDT,NUMCYC
10    FORMAT(3F15.5)
20    FORMAT(2F15.5,E20.7)
30    FORMAT(2F15.5)
40    FORMAT(3I7)
      RETURN
      END
C
C
      SUBROUTINE PRINTP(PHIF,GF,GS,MS,K,MW,XID,U1
     *,U0,SRU1U0,O0,O1,X,L)
      REAL MS,K,MW,L
      WRITE(7,10)
      WRITE(7,11) X,L
      WRITE(7,20) GF,GS,MS
      WRITE(7,30) PHIF,K,MW
      WRITE(7,40) XID,U1,U0,SRU1U0,O0
10    FORMAT(6X,'PROGRAM RESO  RUHR SANDSTONE',//
     *6X,'MATERIAL PROPERTIES',//,6X,'INPUT'/)
20    FORMAT(6X,'TRUE DENSITY, FLUID  ',15X,F10.3,8X,'  G/CC'/
     *6X,'BULK DENSITY, SOLID  ',15X,F10.3,8X,'  G/CC'/
     *6X,'SHEAR MODULUS, SOLID  ',12X,E20.7,'  DYNES/SQ-CM'/)
11    FORMAT(6X,'POSITION IN FORMATION',15X,F10.3,8X,'  CM'/
     *6X,'FORMATION DEPTH',6X,15X,F10.3,8X,'  CM'/)
30    FORMAT(6X,'POROSITY  ',25X,F15.7,'      VOL/VOL'/
     *6X,'PERMIABILITY  ',20X,E20.7,'  SQ-CM'/
     *6X,'VISCOSITY, FLUID  ',16X,E20.7,'  POISE'/)
40    FORMAT(6X,'OUTPUT',//
     *6X,'DRAG COEFFICIENT  ',16X,E20.7,'  DYNE-SEC/CM**4'/
     *6X,'ACCELERATION WAVE SPEED  ',9X,E20.7,'  CM/SEC'/
     *6X,'FROZEN WAVE SPEED  ',15X,E20.7,'  CM/SEC'/
     *6X,'RATIO OF ACCEL BY FROZEN, SQUARED  ',F15.7/
     *6X,'RECIPRICAL CHAR. TIME FOR DIFF.  ',1X,E20.7,'  RAD/SEC'///
     *6X,'OUTPUT OF DECAY EXPONENTS AND NATURAL FREQUENCIES'//)
```

```
      RETURN
      END
C
C
C
C
      SUBROUTINE DISPM(PHI,OMEGA0,OMEGA1,U1,U0,SRU1U0,L,X
     *,NUMPHI,NUMDT,NUMCYC,DUMCYC,PHICYC,DMAX,DSSMAX,RMSMAX,TMAX)
      REAL MCDA,MCDB,MMD,MSA,MSB,L,NUMCYC
      PI=3.14159265
      CALL SSCOMP(PHI,SRU1U0,U1,OMEGA0,OMEGA1,X,L,MSA,MSB)
      DT=2.*PI*ABS(DUMCYC-NUMCYC)/FLOAT(NUMDT)/PHICYC
      T=DUMCYC*2.*PI/PHICYC
C GIVES DT S.T. THE LAST CYCLE OF NUMCYC OF PHICYC IS USED
C THE USER MUST DETERMINE IF VARYING NUMDT INDICATES A PROBABLE
C MAXIMUM HAS BEEN FOUND. COMPARE TO RMSMAX
      ABS3=0.
      ABS4=0.
      RMS3=0.
      RMS4=0.
      SUM1=0.
      SUM=0.
      TMAX=0.
              DO 500 J=1,NUMDT
      T=T+DT
      ABS1=0.
      ABS2=0.
      RMS1=0.
      RMS2=0.
      WMD=0.0000001
      WCD=0.0000001
      WSS=MSA*COS(PHI*T)+MSB*SIN(PHI*T)
      N=1
100   CONTINUE
      GAMMAN= FLOAT(2*N-1)*3.14159265/2./L
      CALL ROOTS(OMEGA0,U1,U0,GAMMAN,XIN,DUM1,DUM2)
```

```
      CALL CALMMD(GAMMAN,PHI,XIN,L,X,OMEGA0,OMEGA1,U1,U0,N,MMD)
      DUM= MMD*EXP(-XIN*T)
      WMD=WMD+DUM
      ABS1=ABS1+ABS(DUM)
      RMS1=RMS1+DUM*DUM
      N=N+1
      IF(ABS(DUM).LT.0.00001.OR.ABS(DUM/WMD).LT..001) GOTO 150
      GOTO 100
150   CONTINUE
      N=1
101   CONTINUE
      GAMMAN=FLOAT(2*N-1)*3.14159265/2./L
      CALL ROOTS(OMEGA0,U1,U0,GAMMAN,XIN,ZETAN,OMEGAN)
      CALL CALMCD(SRU1U0,X,L,N,GAMMAN,ZETAN,OMEGAN,
     *OMEGA0,OMEGA1,PHI,MCDA,MCDB)
      DUM=MCDA*EXP(-ZETAN*T)*COS(OMEGAN*T)+
     *MCDB*EXP(-ZETAN*T)*SIN(OMEGAN*T)
      WCD=WCD+DUM
      DUM1=(MCDA*EXP(-ZETAN*T))**2+(MCDB*EXP(-ZETAN*T))**2
      RMS2=RMS2+DUM1
      ABS2=ABS2+SQRT(ABS(DUM1))
      N=N+1
      IF(ABS(DUM).LT..00001.OR.ABS(DUM/WCD).LT..001) GOTO 200
      GOTO 101
200           CONTINUE
      RMS3=RMS1+RMS2
      RMS3=AMAX1(RMS3,RMS4)
      RMS4=RMS3
      SUM=ABS(WSS+WCD+WMD)
      ABS3=ABS1+ABS2
      ABS3=AMAX1(ABS3,ABS4)
      ABS4=ABS3
      WRITE(5,31) SUM,RMS3,ABS3,T
31    FORMAT(5X,'SUM',F10.3,'RMS',F10.3,'ABS',F10.3,'T',F10.3)
      DMAX=AMAX1(SUM,SUM1)
      IF(SUM.GT.SUM1) TMAX=T
```

```
      SUM1=DMAX
500           CONTINUE
      DSSMAX=SQRT(MSA**2+MSB**2)
      RMSMAX=SQRT(RMS3+DSSMAX*DSSMAX)
      RETURN
      END
C
C
      SUBROUTINE CALPHI(OMEGA0,OMEGA1,U1,U0,L,NUMPHI,PHIRS)
      DIMENSION PHIRS(20)
      REAL L
      NDUM=2*NUMPHI
              DO 100 I=1,NUMPHI
      GAMMAN=3.14159265*FLOAT(2*I-1)/2./L
      CALL PHIRES(OMEGA0,OMEGA1,U0,L,I,PHIR)
      IDUM=NUMPHI+I
      PHIRS(IDUM)=PHIR
      CALL ROOTS(OMEGA0,U1,U0,GAMMAN,DUM1,DUM2,OMEGAN)
      PHIRS(I)=OMEGAN
100           CONTINUE
      RETURN
      END
C FIRST 2*NUMPHI CD RESONANCES
C CALCULATES THE FIRST NUMPHI CD AND SS RESONANCES
C
C
      SUBROUTINE ROOTS(OMEGA0,U1,U0,GAMMAN,XIN,ZETAN,OMEGAN)
      DIMENSION A(4),B(4),C(4),D(4)
C LIN-BAIRSTOW'S METHOD
      N=3
      N1=N+1
      N2=N+2
      DO 12 J=1,N1
      A(J)=0.
      B(J)=0.
      C(J)=0.
```

```
      D(J)=0.
12    CONTINUE
      A(4)=1.0
      A(3)=OMEGA0
      A(2)=U1*U1*GAMMAN*GAMMAN
      A(1)=U0*U0*GAMMAN*GAMMAN*OMEGA0
200   R=A(2)/A(3)
      S=A(1)/A(3)
220   B(N1)=A(N1)
      C(N1)=0.
      D(N1)=0.
      N=N1-1
      B(N)=A(N)-R*B(N1)
      C(N)=-B(N1)
      D(N)=0.
      NM1=N1-2
      DO 320 I=3,NM1
      NDUM=N1-I
      NDUM2=N1-I+1
      NDUM3=N1-I+2
      B(NDUM)=A(NDUM)-R*B(NDUM2)-S*B(NDUM3)
      C(NDUM)=-B(NDUM2)-R*C(NDUM2)-S*C(NDUM3)
      D(NDUM)=-B(NDUM3)-S*D(NDUM3)-R*D(NDUM2)
320   CONTINUE
      R1=A(2)-R*B(3)-S*B(4)
      S1=A(1)-S*B(3)
      T=-B(3)-R*C(3)-S*C(4)
      U=-B(4)-S*D(4)-R*D(3)
      V=-S*C(3)
      W=-B(3)-S*D(3)
      R2=(-R1*W+S1*U)/(T*W-U*V)
      S2=(-T*S1+V*R1)/(T*W-U*V)
      S=S+S2
      R=R+R2
      IF(ABS(R2).LT.0.000001) GOTO 450
      GOTO 220
```

```
450     G=R*R-4.*S
490     ZETAN=R/2.
        OMEGAN=SQRT(-G)/2.
500     N1=N1-2
        DO 550 J=1,N1
        I=N1-J+1
        IDUM=I+2
        A(I)=B(IDUM)
550     CONTINUE
610     NM1=N1-1
        XIN=A(NM1)/A(N1)
        RETURN
        END
C THE ROOTS ARE -XIN AND -ZETAN +/- iOMEGAN RAD/SEC
C THIS ROUTINE IS A MODIFIED FORM OF A BASIC PROGRAM GIVEN
C IN HOVANESSIAN AND PIPES, DIGITAL COMPUTER METHODS IN ENGINEERING
C 1969, MC GRAW-HILL PP140.
C
C
C
C
        SUBROUTINE PROP(PHIF,GAMMAF,GAMMAS,MUS,K,MUW,
     *XID,U1,U0,SRU1U0,OMEGA0,OMEGA1)
        REAL MUS,MUW,K
        XID= PHIF*PHIF*MUW/K
        RHOF=GAMMAF*PHIF
        RHOS=GAMMAS
C BULK DENSITY FOR THE SOLID IS INPUT
        U1=SQRT(MUS/RHOS)
        U0=SQRT(MUS/(RHOS+RHOF))
        SRU1U0=1.+RHOF/RHOS
        OMEGA0=XID*(1./RHOS+1./RHOF)
        OMEGA1=OMEGA0/SRU1U0
        RETURN
        END
C SRU1U0 IS THE RATIO OF U1 BY U0 SQUARED
```

```
C UNITS MAY BE ANY CONSISTANT SET
C PHIF IS THE POROSITY
C GAMMAF AND GAMMAS ARE THE TRUE DENSITIES OF THE FLUID AND SOLID
C MUS IS THE SHEAR MODULUS OF THE SOLID DYNE/SQ.CM.
C MUW IS THE VISCOSITY OF THE FLUID IN POISE
C K IS THE PERMIABILITY SQ.CM.
C XID IS THE DRAG COEFFICIENT IN DYNE-SEC/CM**4
C U1 IS THE ACC. WAVE SPEED CM/SEC
C U0 IS THE FROZEN WAVE SPEED CM/SEC
C OMEGA0 IS THE RECIPRICAL CHAR. TIME FOR DIFFUSION CM/SEC
C OMEGA1 RAD/SEC
C
C
        SUBROUTINE PHIRES(OMEGA0,OMEGA1,U0,L,N,PHIR)
        REAL L
        F(X)=((1.+(X/OMEGA0)**2)/(1.+(X/OMEGA1)**2))**.25
     **COS((ATAN2(X,OMEGA0)-ATAN2(X,OMEGA1))*0.5)*X/U0
     *-3.14159265*FLOAT(2*N-1)/L/2.
        PHI0=3.14159265*FLOAT(N)*U0/L
C FIRST GUESS
C START WITH NEWTON-RAPHSON F.D. METHOD
        H=PHI0*1.E-7
        DUM1=F(PHI0)
        DUM2=F(PHI0+H)
        A0=(DUM2-DUM1)/H
        PHI1=PHI0-DUM1/A0
C USE THE SECANT METHOD UNTIL F NEAR ZERO
100     TEST=F(PHI1)
        IF(ABS(TEST).LT.1.E-5) GOTO 1000
        A0=(DUM1-TEST)/(PHI0-PHI1)
        DUM1=TEST
        PHI0=PHI1
        PHI1=PHI0-TEST/A0
        GOTO 100
1000    PHIR=PHI1
        RETURN
```

```
      END
      SUBROUTINE CDPHI(PHI,SRU1U0,OMEGA0,OMEGA1,C,D)
      DUM1=((1.+(PHI/OMEGA0)**2)
     */(1.+(PHI/OMEGA1)**2))**.25
      DUM2=(ATAN2(PHI,OMEGA0)-ATAN2(PHI,OMEGA1))*0.5
      C=-PHI*DUM1*SIN(DUM2)*SQRT(SRU1U0)
      D=PHI*DUM1*COS(DUM2)*SQRT(SRU1U0)
      RETURN
      END
C
C
C
      SUBROUTINE CALMCD(SRU1U0,X,L,N,GAMMAN,ZETAN,OMEGAN,OMEGA0,
     *OMEGA1,PHI,MCDA,MCDB)
      REAL L,MCDA,MCDB
      DUMM=OMEGA1-OMEGA0
      DUM0=OMEGA0-ZETAN
      DUM1=OMEGA1-ZETAN
      DUMN=OMEGAN**2+ZETAN**2
      DUM0B=DUM0**2+OMEGAN**2
      DUM1B=DUM1**2+OMEGAN**2
      C=(PHI**2-(OMEGAN)**2)
      C=C+ZETAN**2
      D=-2.*ZETAN*OMEGAN
      A=.5*DUMM*(DUM0*DUM1-(OMEGAN)**2)/DUM0B/DUM1B
      A=A-ZETAN/DUMN
      B=-OMEGAN*.5*DUMM*(OMEGA1+OMEGA0-2.*ZETAN)/DUM0B/DUM1B
      B=B-OMEGAN/DUMN
      PART1=(A*C-B*D)**2
      PART2=(D*A+B*C)**2
      PART2=PART2+PART1
      MCDA=(A*C-B*D)/PART2
      MCDB=(D*A+B*C)/PART2
      PI=3.14159265
      DUM=4.*PHI*COS(X*FLOAT(2*N-1)*PI/2./L)/FLOAT(2*N-1)/PI
      IF(MOD(N,2).NE.0) DUM=-DUM
```

```
      MCDA=MCDA*DUM
      MCDB=MCDB*DUM
C MCDA IS COS TERM MCDB IS SIN TERM
      RETURN
      END
C
C
C
      SUBROUTINE CALMMD(GAMMAN,PHI,XIN,L,X,OMEGA0,OMEGA1,U1,U0,N,MMD)
      REAL MMD,L
      DUMM=OMEGA1-OMEGA0
      DUMN=XIN**2+PHI**2
      DUM0=OMEGA0-XIN
      DUM1=OMEGA1-XIN
      DUM2=(U1*U1-U0*U0)*GAMMAN*GAMMAN/OMEGA0
      DUM0=AMAX1(DUM0,DUM2)
C TO MAKE SURE DUM0 IS NEVER ZERO
C
      PI=3.14159265
      DUMARG=PI*FLOAT(2*N-1)*X/2./L
      PART1=2.*PHI*COS(DUMARG)/PI/FLOAT(2*N-1)
      PART2=DUMM*XIN*XIN/2./DUM0/DUM1
      PART2=PART2-XIN
      PART2=PART2-PHI*PHI/XIN
      PART2=PART2+PHI*PHI*DUMM/2./DUM0/DUM1
      MMD=PART1/PART2
      IF(MOD(N,2).EQ.0) MMD=-MMD
      RETURN
      END
C THE MAGNITUDE OF EQUATION 2.118
C
C
C
      SUBROUTINE SSCOMP(PHI,SRU1U0,U1,OMEGA0,OMEGA1,X,L,MSA,MSB)
      REAL MSA,MSB,L
      COSH(X)=(EXP(X)+EXP(-X))*.5
```

```
      SINH(X)=(EXP(X)-EXP(-X))*.5
      CALL CDPHI(PHI,SRU1U0,OMEGA0,OMEGA1,C,D)
      X1=X*C/U1
      Y1=X*D/U1
      X2=L*C/U1
      Y2=L*D/U1
      A=COSH(X1)*COS(Y1)
      B=SINH(X1)*SIN(Y1)
      C=COSH(X2)*COS(Y2)
      D=SINH(X2)*SIN(Y2)
      DENOM=(SINH(X2))**2+(COS(Y2))**2
      MSA=(B*C-A*D)/DENOM
      MSB=(A*C+B*D)/DENOM
C MSA IS COS TERM MSB SIN TERM
      RETURN
      END
C
```